Journal of Medicinal Chemistry Article

J. Med. Chem. **2009,** *52,* 5449–5461 **5449**
DOI: 10.1021/jm900639u

Efficacious 11β-Hydroxysteroid Dehydrogenase Type I Inhibitors in the Diet-Induced Obesity Mouse Model

Zhao-Kui Wan,*[,†] Eva Chenail,[†] Jason Xiang,[†] Huan-Qiu Li,[†] Manus Ipek,[†] Joel Bard,[†] Kristine Svenson,[†] Tarek S. Mansour,[†] Xin Xu,[‡] Xianbin Tian,[‡] Vipin Suri,[§] Seung Hahm,[§] Yuzhe Xing,[§] Christian E. Johnson,[§] Xiangping Li,[§] Ariful Qadri,[§] Darrell Panza,[§] Mylene Perreault,[§] James F. Tobin,[§] and Eddine Saiah[†]

[†]*Chemical Sciences and* [‡]*Drug Safety and Metabolism and* [§]*Metabolic Diseases, Wyeth Research, 200 Cambridge Park Drive, Cambridge, Massachusetts 02140*

Received May 14, 2009

Cortisol and the glucocorticoid receptor signaling pathway have been implicated in the development of diabetes and obesity. The reduction of cortisone to cortisol is catalyzed by 11β-hydroxysteroid dehydrogenase type I (11β-HSD1). 2,4-Disubsituted benzenesulfonamides were identified as potent inhibitors of both the human and mouse enzymes. The lead compounds displayed good pharmacokinetics and ex vivo inhibition of the target in mice. Cocrystal structures of compounds **1** and **20** bound to human 11β-HSD1 were obtained. Compound **20** was found to achieve high concentrations in target tissues, resulting in 95% inhibition in the ex vivo assay when dosed with a food mix (0.5 mg of drug per g of food) after 4 days. Compound **20** was efficacious in a mouse diet-induced obesity model and significantly reduced fed glucose and fasted insulin levels. Our findings suggest that 11β-HSD1 inhibition may be a valid target for the treatment of diabetes.

Introduction

More than 150 million people worldwide have diabetes, and this number is expected to rise to 300 million by the year 2025. In the U.S., it is estimated that 21 million people have diabetes, and in some areas of the country, the prevalence is as high as 50%.[1] Metabolic syndrome is a prediabetic state that consists of glucose intolerance, abdominal obesity, dyslipidemia, hypertension, insulin resistance, and inflammatory or prothrombotic states.[2] As metabolic syndrome progresses to diabetes, complications associated with this disorder become more prominent and include cardiovascular disease, diabetic retinopathy, kidney failure, and nerve damage.

A number of therapies are presently available for treating diabetes. These include insulin secretagogues, insulin sensitizers, and modulators of glucose uptake and production. Despite these advances, there is an acute need for improved therapies that target the various biological pathways involved in this disease.[3]

Recent investigations have implicated aberrant glucocorticoid receptor (GR[a]) signaling in the development of several phenotypes associated with metabolic syndrome. Glucocorticoid hormones are key metabolic regulators. The major activator of the GR in humans is cortisol, and the adrenal cortex is the major source of circulating cortisol. GR signaling depends not only on the circulating cortisol levels but also on the intracellular generation of cortisol through reduction of cortisone, the inactive glucocorticoid.[4] The reduction reaction is catalyzed by 11β-hydroxysteroid dehydrogenase type 1 (11β-HSD1) with the concomitant oxidation of reduced β-nicotinamide adenine dinucleotide phosphate (NADPH), while cortisone itself is generated by the action of 11β-hydroxysteroid dehydrogenase type 2 (11β-HSD2) on cortisol using β-nicotinamide adenine dinucleotide phosphate (NADP) as a cofactor.[2] These two enzymes have very different expression profiles: 11β-HSD1 levels are highest in liver, adipose tissues, and the central nervous system, whereas 11β-HSD2 is expressed in kidney, colon, and other tissues.[2]

Transgenic mice overexpressing 11β-HSD1 in adipose tissue show several features of metabolic syndrome including abdominal obesity, glucose intolerance, dyslipidemia, and hypertension.[5] 11β-HSD1 activity in adipose tissue also correlates positively with body mass index (BMI), fat percentage, and fasting glucose and insulin levels in humans. In addition, liver-specific overexpression of 11β-HSD1 in transgenic mice causes insulin resistance without obesity.[6] 11β-HSD1 knockout mice demonstrate reduction in body weight, decreased low-density lipoprotein (LDL) and triglyceride levels, increased high density lipoprotein (HDL) levels, and increased insulin sensitivity when maintained on a high fat diet.[7] The combined findings from the knockout mice and the transgenic mice make a compelling case for evaluating 11β-HSD1 inhibitors for the treatment of diabetes and the metabolic syndrome.

There are reports in the literature of several classes of potent and selective 11β-HSD1 inhibitors,[8] a few of which display in

*To whom correspondence should be addressed. Phone: 617-665-5635. Fax: 617-665-5682. Email: zwan@wyeth.com.

[a] Abbreviations: 11β-HSD1, 11β-hydroxysteroid dehydrogenase type 1; 11β-HSD2, 11β-hydroxysteroid dehydrogenase type 2; DIO, diet-induced-obesity; PK, pharmacokinetics; SAR, structure−activity relationship; NADP, β-nicotinamide adenine dinucleotide phosphate; NADPH, reduced β-nicotinamide adenine dinucleotide phosphate; CHO cell, Chinese hamster ovary cell; UDPGA, uridine diphosphoglucuronic acid; BMI, body mass index; HDL, high density lipoprotein; LDL, low density lipoprotein; GR, glucocorticoid receptor; HLM, human liver microsome; MLM, mouse liver microsome; RLM, rat liver microsome.

Published on Web 08/10/2009

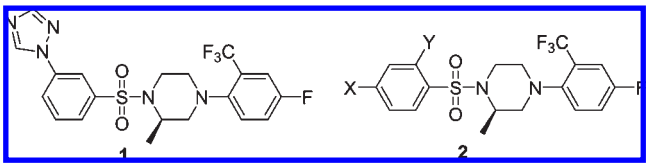

Figure 1. Previously reported bezenesulfonamide 11β-HSD1 inhibitor **1** and general structure of benzenesulfonamides described in this study (**2**).

vitro efficacy in animal models related to diabetes. Biovitrum reported a thiazole-based selective 11β-HSD1 inhibitor that reduced plasma glucose levels and improved glucose tolerance in murine models of obesity and type 2 diabetes ($Lep^{ob/ob}$ and KKA^{y}, respectively) when dosed at 200 mg/kg bid.[9] Thienyl derivatives also showed a similar effect.[10] Merck reported triazole-based 11β-HSD1 inhibitors that reduced food intake, body weight, fasting glucose, and insulin levels in the diet-induced obesity (DIO) mouse model studies when orally dosed at 20 mg/kg bid.[11] Abbott researchers described an adamantyl amide that lowered plasma glucose levels in the ob/ob mouse model in a three-week study with oral dosing at lowest dose of 30 mg/kg bid.[12] Additionally, the adamantine lactam 11β-HSD1 inhibitor from Abbott induced weight loss and lowered plasma insulin levels in DIO mice when orally dosed at 30 mg/kg bid for 14 days. Plasma triglyceride levels were notably normalized.[13] Recently disclosed Pfizer aminopyridine analogue PF-915275 significantly lowered plasma insulin levels (by 54 and 60%, respectively) at 1 and 3 mg/kg, 8 h after dosing in normal cynomolgus monkeys.[14] Interestingly, neither plasma glucose nor lipid levels were altered with the treatment.

We previously disclosed a series of benzenesulfonamides as potent and selective 11β-HSD1 inhibitors.[15] We described our efforts to optimize the piperazine ring and the right-hand portion of the molecule along with detailed structure−activity relationship (SAR) efforts on the meta position of the left side phenyl ring. Compound **1** (Figure 1) was reported to have an $IC_{50} = 26$ nM against human 11β-HSD1 and showed efficacy in the cortisone-induced hyperinsulinemia rat model by lowering insulin levels after 7 days of treatment.[15] Compound **1** displayed low to moderate microsomal stability (12 min in presence of mouse microsomes and 17 min in presence of human microsomes). Herein, we wish to report our efforts toward further optimization by focusing on the ortho- and para-positions on the left side phenyl ring (structure **2**, Figure 1). We report the ex vivo activity and pharmacokinetic profile of selected compounds and encouraging in vitro efficacy results from DIO studies in mice.

Crystal Structure and Optimization Strategy. An X-ray cocrystal structure of compound **1** bound to human 11β-HSD1 was obtained by X-ray crystallography to a resolution of 2.3 Å (Figure 2). Analysis of the binding mode revealed some key interactions. The trifluoromethyl group sits in a hydrophobic pocket formed by the side chains of L126 and A226 and the backbone of S125. One of the sulfone oxygens makes a hydrogen bond with the backbone nitrogen of A172. The unsubstituted edge of the piperazine ring has close van der Waals interactions with Y183. There are additional van der Waals interactions between the benzylic fluoro substituent and T124 and I121 as well as with the NADP cofactor. The phenyltriazole group of compound **1** contributes to π-stacking interactions with Y177 and extends to make van der Waals contacts with P178. Further examination of the

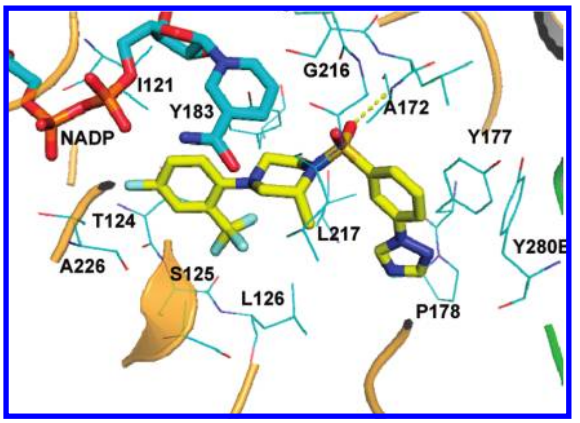

Figure 2. Crystal structure of **1** bound to human 11β-HSD1 (PDB code: 3H6K). Crystal structure of **1** bound to 11β-HSD1. The inhibitor is shown with yellow carbons, the NADP+ cofactor is shown with cyan carbons. Residues containing atoms within 4 Å of the inhibitor are shown with thin cyan bonds. Secondary structure elements from monomer A of the 11β-HSD1 protein are shown in orange, while those from monomer B are shown in green. Figure generated with Pymol.[26]

Scheme 1. Synthesis of Compounds **7**−**10**[a]

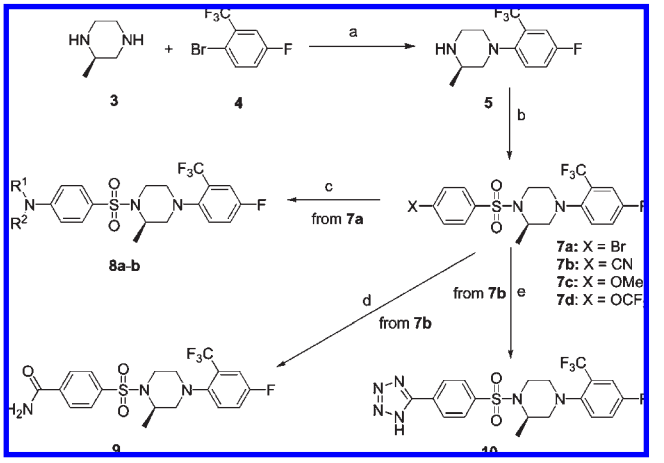

[a] Reagents and conditions: (a) $Pd_2(dba)_3$, BINAP, *t*-BuONa, toluene; (b) $ArSO_2Cl$ (**6**), diisopropylethylamine, CH_2Cl_2; (c) R^1R^2NH, $Pd_2(dba)_3$, BINAP, *t*-BuONa, toluene; (d) KOH, *t*-BuOH; (e) NaN_3, $Et_3N \cdot HCl$, toluene.

binding pocket on the left side of the molecule **1** (as drawn in Figure 1) revealed an opportunity for introducing groups at the ortho and para positions of the benzenesulfonamide. There is a depression in the van der Waals surface of the protein adjacent to G216 that might be accessed by small groups at the ortho position of the benzene sulfonamide. The para position points toward a solvent exposed cleft at the interface between dimeric partners in the enzyme complex, suggesting that it could accept potentially larger and more polar solubilizing substituents that could lead to improved physicochemical and ADME properties. Thus we embarked in SAR studies focused on the ortho and para positions of the benzenesulfonamide.

Chemistry. Scheme 1 depicts the synthesis of para-substituted benzenesulfonamides. Buchwald amination[16] of bromide **4** with (*R*)-methylpiperazine **3** selectively provided the desired product **5** in excellent yield.[15] Reaction of **5** with various sulfonyl chlorides (**6**) in the presence of diisopropylethylamine efficiently gave sulfonamides **7a**−**d**. A second

Scheme 2. General Synthesis of 2-Chloro or Fluoro-4-amino Analogues **12**−**15**[a]

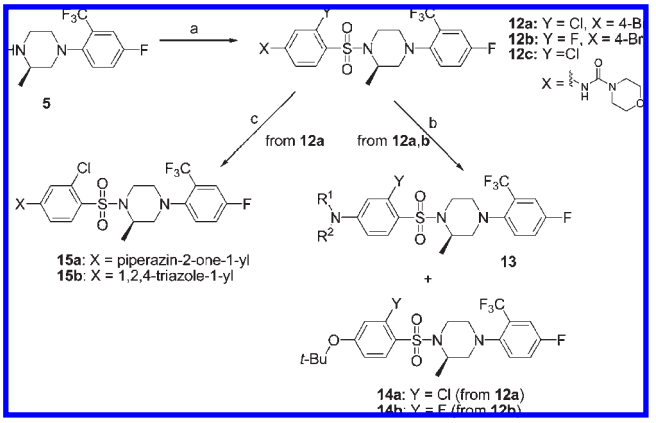

[a] Reagents and conditions: (a) $Ar'SO_2Cl$ (**11**), diisopropylethylamine, CH_2Cl_2. (b) R^1R^2NH, $Pd_2(dba)_3$, BINAP, *t*-BuONa, toluene. (c) For **15a**: (i) *tert*-butyl 3-oxopiperazine-1-carboxylate, CuI, K_3PO_4, *trans*-*N*, *N*′-dimethylcyclohexane-1,2-diamine; diglyme; (ii) TFA, CH_2Cl_2; for **15b**: 1,2,4-triazole, CuI, K_2CO_3, NMP.

Scheme 3. General Synthesis of 2-Chloro-4-alkoxy Analogues **16**−**18**[a]

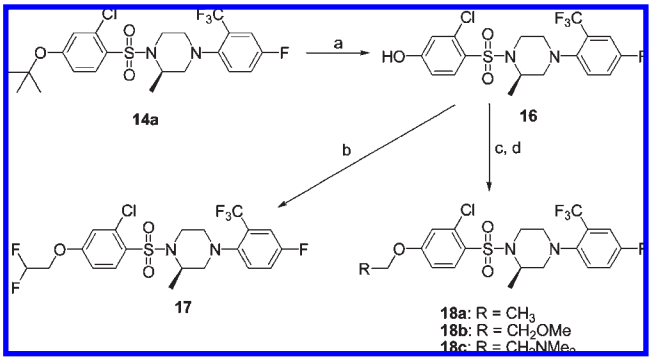

[a] Reagents and conditions: (a) TFA, CH_2Cl_2; (b) $ClCF_2CO_2Me$, Cs_2CO_3, DMF/H_2O; (c) for **18a**: DEAD, PPh_3, THF; (d) for **18c** and **18c** DEAD, PPh_3, R-CH_2OH, THF.

Buchwald amination of bromide **7a** with secondary amines in the presence of $Pd_2(dba)_3$ and *t*-BuONa in toluene provided the desired 4-amino benzenesulfonamides **8a** and **8b** in good yields. Treatment of the cyano derivative **7b** with KOH in *t*-BuOH provided 4-amide analogue **9** in near quantitative yield. Reaction of **7b** with NaN_3 led to formation of the desired tetrazole analogue **10** in 61% isolated yield.

2-Chloro- and 2-fluoro-4-amino-analogues **13** and **15** were synthesized as shown in Scheme 2. 4-*tert*-Butyl ethers **14a** (Y = Cl) and **14b** (Y = F) were occasionally isolated in variable yields. The formation of these ether analogues was likely due to the presence of *t*-BuONa in the reaction mixture. Copper catalyzed C−N bond formation of the 4-bromobenzenesulfonamide **12a** (X = Br) with nitrogen-containing heterocycles led to the corresponding 4-amino-heterocyclic benzenesulfonamides **15a** and **15b**.

2-Chloro-4-alkoxy-analogues were also prepared (Scheme 3). *t*-Bu ether **14a** was converted to phenol **16** in the presence of trifluoroacetic acid (TFA). Alkylation of **16** with methyl-2-chloro-2,2-difluoroacetate led to **17**. Mitsunobu reaction with alkyl alcohols furnished analogues **18b** and **18c**. Interestingly, compound **18a** was formed when the Mitsunobu reaction was run without the addition of ethanol. The ethyl group in the final product **18a** was likely derived from diethyl azodicarboxylate (DEAD). Scheme 4 shows the syntheses of the 4-amido analogue **20.** This analogue was prepared using similar procedures described for the preparation of compounds **9** in Scheme 1.

Scheme 4. Synthesis of 2-Chloro-4-carbon Analogues **19** and **20**[a]

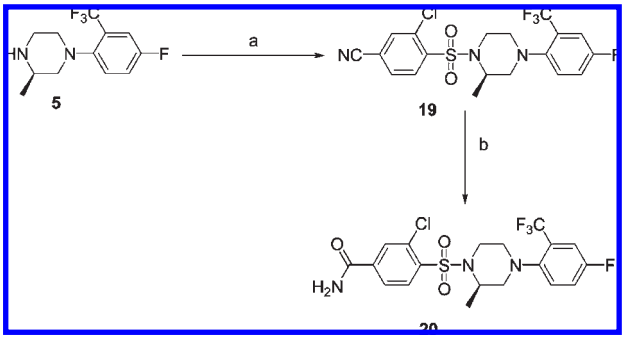

[a] Reagents and conditions: (a) 2-chloro-4-cyanobenzene-1-sulfonyl chloride, diisopropylethylamine, CH_2Cl_2; (b) KOH, *t*-BuOH.

Results and Discussion

Structure−Activity Relationship (SAR). Examination of the binding mode of compound **1** revealed the possibility of further optimization at the para position of the sulfonamide phenyl ring. Of particular interest was the possibility of introducing polar groups, as suggested by the crystal structure information, to improve the physicochemical and ADME profiles of the molecules. Synthesized compounds were first evaluated in a cell-based assay using a stable Chinese hamster ovary (CHO) cell line expressing 11β-HSD1. The assay was run in duplicate; the compounds were tested in 11-point dilutions and the standard error of IC_{50} was $< 10\%$ (See Experimental Section for assay protocols). Table 1 summarizes the in vitro data for selected compounds with substitutions at the para position. As predicted from the crystal structure, substitution at the para position was well tolerated. Compounds such as the cyano analogue **7b** and the morpholino analogue **8b** retained good potency (IC_{50} = 10 nM). Other analogues such as the alkyl ethers **7c** and **7d**, the piperidine **8a**, and the amide **9** also displayed good inhibitory activity against the human enzyme. Introduction of a weakly acidic tetrazole at the para position (compound **10**) led to a significant drop in potency. Most para-substituted analogues displayed good human microsomal stability ($t_{1/2} > 30$ min) and moderate mouse microsomal stability.

Once we established that the para position of the benzenesulfonamide series tolerates a range of substituents, we expanded the scope of our investigations by exploring 2,4-disubstituted benzenesulfonamides. Several groups, such as Cl, F, MeO, and CO_2H, were introduced at the ortho position. In general, the ortho Cl group was found to offer the best balance in terms of potency and ex vivo activity (data not shown). The remaining of the discussion will focus on ortho Cl analogues with various substituents at the para position. Table 2 summarizes the SAR for this series of analogues.

Most of the 2-chloro-4-amino analogues showed good inhibition of human and mouse 11β-HSD1 with IC_{50} values in the low nM range. For example, the tertiary amine analogues **13a**

Table 1. Inhibitory Activities and Microsomal Stabilities of Compounds **7**−**10**

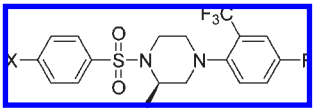

compound	X	h-HSD1 IC_{50} (μM)[a]	m-HSD1 IC_{50} (μM)[a]	m-HSD1+ h-serum IC_{50} (μM)[a, b]	MLM $t_{1/2}$ (min)	HLM $t_{1/2}$ (min)
7a	Br	0.028	-	0.011	14	> 30
7b	CN	0.010	0.636	0.467	15	18
7c	OMe	0.020	-	0.016	3	7
7d	OCF_3	0.023	0.016	0.054	12	> 30
8a		0.019	-	0.661	9	> 30
8b		0.010	0.069	0.368	15	> 30
9		0.063	0.010	0.025	21	> 30
10		0.674	2.337	> 10	14	> 30

[a] The assay was done in duplicates; the compounds were tested in 11-point dilutions and the standard error of IC_{50} was < 10%; the lower threshold of this assay is 10 nM. [b] 10% (v/v) human serum was added to the cell culture media.

Table 2. Inhibitory Activities and Microsomal Stabilities of Compounds **12a** and **13a**−**i**

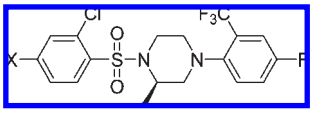

compound	X	h-HSD1 IC_{50} (μM)[a]	m-HSD1 IC_{50} (μM)[a]	m-HSD1+ h-serum IC_{50} (μM)[a, b]	MLM $t_{1/2}$ (min)	HLM $t_{1/2}$ (min)
12a	Br	0.010	0.010	0.010	21	> 30
13a		0.015	0.010	0.010	2	-
13b		0.011	0.012	0.010	5	-
13c		0.097	-	0.276	6	21
13d		0.050	0.015	0.010	>30	>30
13e		0.074	0.017	0.022	-	>30
13f		0.015	0.010	0.010	>30	>30
13g		0.010	0.010	-	14	>30
13h		0.010	0.010	0.016	> 30	>30
13i		0.017	0.010	0.010	13	>30

[a] The assay was done in duplicates; the compounds were tested in 11-point dilutions and the standard error of IC_{50} was < 10%; the lower threshold of this assay is 10 nM. [b] 10% (v/v) human serum was added to the cell culture media.

and **13b** had IC_{50} values in the 10 nM range for human and mouse 11β-HSD1. Alkyl amines such as **13a**, **13b**, and **13c** showed poor microsomal stability ($t_{1/2}$ = 2−6 min for mouse microsomes). Introduction of one or two fluoro substituents at the 4-position of the piperidine ring (**13d** and **13e**, respectively) led to a significant improvement in the microsomal stability ($t_{1/2}$ > 30 min) with a comparable potency versus the human enzyme compared to the *des*-fluoro analogue **13c**. Introduction of polar groups at the piperidine 4-position was also well tolerated: **13f**−**i** all showed low nM inhibition of human and mouse 11β-HSD1 and good microsomal stability in human liver microsomes ($t_{1/2}$ > 30 min).

Table 3. Inhibitory Activities and Microsomal Stabilities of Compounds **12c**, **13j**−**p**, and **15a**−**b**

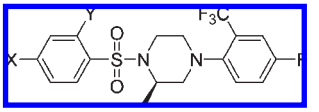

compound	X	Y	h-HSD1 IC_{50} (μM)[a]	m-HSD1 IC_{50} (μM)[a]	m-HSD1+ h-serum IC_{50} (μM)[a, b]	MLM $t_{1/2}$ (min)	HLM $t_{1/2}$ (min)
13j		Cl	0.010	0.010	0.010	14	>30
13k		F	0.011	0.010	0.032	22	>30
13l		Cl	0.185	0.088	0.194	7	>30
12c		Cl	0.115	0.071	>10	>30	>30
13m		Cl	0.136	0.128	0.672	18	>30
13n		Cl	0.639	0.010	0.083	>30	>30
13o		Cl	0.010	0.010	0.010	>30	>30
13p		Cl	0.010	0.010	0.010	13	>30
15a		Cl	0.018	-	-	10	21
15b		Cl	0.010	0.010	0.016	>30	26

[a] The assay was done in duplicates; the compounds were tested in 11-point dilutions and the standard error of IC_{50} was < 10%; the lower threshold of this assay is 10 nM. [b] 10% (v/v) human serum was added to the cell culture media.

Further exploration of the para position led to compounds in Table 3. Replacing the piperidine ring in **13c** with a morpholino group led to analogue **13j**. Compound **13j** was found to be equipotent to its parent *des*-chloro analogue **8b** against human 11β-HSD1 but displayed a 36-fold improvement against the mouse enzyme in the presence of serum when compared to the *des*-chloro analogue **8b**. The *ortho*-fluoro analogue **13k** also showed strong inhibitory activity against the human 11β-HSD1 (IC_{50} = 11 nM). The 2,6-dimethyl morpholino analogue **13l** showed a decrease in potency against both the human and mouse enzymes. The morpholino urea analogue **12c** also showed a significant drop in potency against both human and mouse enzymes but displayed good microsomal stability ($t_{1/2}$ > 30 min) in the presence of human and mouse liver microsomes. Piperazine analogues **13m** and **13n** showed 14- and 64-fold drops in potency against human 11β-HSD1, respectively, when compared to the morpholino analogue **13j**, suggesting that positively charged moieties are not well tolerated at this

Table 4. Inhibitory Activities and Microsomal Stabilities of Compounds **14a**, **16**, **17**, **18a−c**, and **19−20**

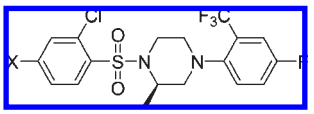

compound	X	h-HSD1 IC_{50} (μM)[a]	m-HSD1 IC_{50} (μM)[a]	m-HSD1+ h-serum IC_{50} (μM)[a, b]	MLM $t_{1/2}$ (min)	HLM $t_{1/2}$ (min)
14a	O-*t*-Bu	0.040	0.013	0.127	9	-
16	OH	0.050	0.012	0.038	4	-
17	$O\text{-}CHF_2$	0.018	0.010	0.010	9	30
18a	O-Et	0.063	0.012	0.020	2	22
18b	$O(CH_2)_2OMe$	0.031	0.010	0.048	7	-
18c	$O(CH_2)_2NMe_2$	0.092	0.010	0.010	18	>30
19	CN	0.016	0.010	0.398	13	14
20		0.010	0.010	0.010	> 30	> 30

[a] The assay was done in duplicates; the compounds were tested in 11-point dilutions and the standard error of IC_{50} was < 10%; the lower threshold of this assay is 10 nM. [b] 10% (v/v) human serum was added to the cell culture media.

position. The less basic piperazinones **13p** and **15a** retained the same level of potency against the human enzyme, as did the neutral sulfone **13o** and the triazole analogue **15b**. Most of these analogues had good stability in human and mouse microsomes.

In addition to 2-chloro-4-amino analogues **13a−j**, **13l−p**, and **15a−b**, we also explored 2-chloro-4-alkoxy-disubstituted species (Table 4). All of the 2-chloro-4-alkyoxy analogues showed moderate to good inhibitory activity against both the human and mouse enzymes. Compounds **17** and **18c** have good microsomal stability against human microsome ($t_{1/2}$ > 30 min) but in general the mouse microsomal stability was poor. Examples of 2-chloro-4-carbon analogues include **19** to **20**. The amido analogue **20** was also potent against both the human and mouse enzymes and displayed excellent microsomal stability ($t_{1/2}$ > 30 min).

The structure of compound **20** bound to human 11β-HSD1 was also obtained by X-ray crystallography to a 2.2 Å resolution (Figure 3). We observed that compounds **1** and **20** bind in a similar fashion: in both structures, one of the sulfone oxygens makes a hydrogen bond with the backbone nitrogen of A172. However, compounds **1** and **20** also exhibit distinct differences in their protein interactions due to the differences in benzylic substitution pattern. As a result, different induced fit effects on the binding pocket are observed. The dihedral angle of the bond joining the sulfonamide sulfur to the phenyl ring differs by 21° between the two compounds. This rotation is necessary to accommodate meta versus para substitutions with minimal remodeling of the pocket. In compound **20**, the phenyl ring, which the chloro group attaches to, rotates so that the ortho chloro group can participate, along with neighboring ring atoms, in van der Waals interactions with Y177. Electrostatic interaction between the amide oxygen and the hydroxyl of Y177 may also contribute to the binding of this compound. We also observed an additional interaction between the ortho Cl group with the piperazine nitrogen through van der Waals interaction, which could further stabilize the bound conformation of the inhibitor.

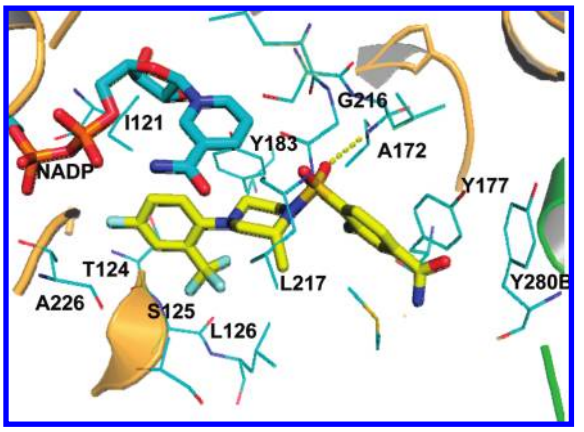

Figure 3. Crystal structure of **20** bound to human 11β-HSD1 (PDB code: 3HFG).

Table 5. Selected Mouse ex vivo Data[a]

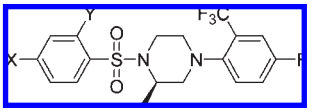

entry	compd	Y	X	Liver inh.[b]	Epi fat inh.[b]
1	**8b**	H		<10%[c]	-
2	**9**	H		-	25%
3	**13h**	Cl	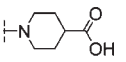	59%	40%
4	**13i**	Cl	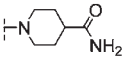	50%	-
5	**13j**	Cl		56%	54%
6	**13k**	F		<10%	<10%
7	**20**	Cl		-	80%

[a] See Experimental Section for assay protocols; [b] po at 10 mg/kg. [c] po at 50 mg/kg.

It is highly desirable that 11β-HSD1 inhibitors show selectivity against 11β-HSD2 bacause mutation of 11β-HSD2 is known to cause mineralocorticoid excess and hypertension due to kidney mineralocoticoid receptor activation.[17] The 11β-HSD1 inhibitors described in this report showed no activity against human 11β-HSD2 when tested at 100 μM.

Ex vivo and Pharmacokinetics Results. A selected number of compounds were evaluated in the ex vivo assays and 11β-HSD1 inhibition was measured in liver, fat, or both. Mice were sacrificed 5 h after oral dosing. The liver and epididymal fat were collected, and the whole tissue was incubated in the presence of [^{3}H]-cortisone in the media. After 30 min, cortisol levels were measured to determine the level of compound inhibition from [^{3}H]-cortisone to [^{3}H]-cortisol. The liver and/or fat ex vivo data are summarized in Table 5.

Table 6. Selected PK Profiles[a]

	iv[b]				po[c]				
compd	Cl (mL min^{-1} kg^{-1})	Vss (L kg^{-1})	AUC (h ng mL^{-1})	$t_{1/2}$ (h)	*C*max (ng mL^{-1})	t_{max} (h)	AUC (h ng mL^{-1})	$t_{1/2}$ (h)	*F* (%)
9	19	3.7	1776	3.2	2833	0.5 h	11279	2.2	43
13h	9	2.0	3512	3.5	6882	1	20507	2.6	100
13i	11	4.6	3147	7.4	913	1	5539	2.9	35
13j	55	4.5	609	2.1	361	0.5	1063	3.8	12
20	5	2.6	6738	7.3	1438	4.0	17001	7.2	50

[a] See Experimental Section for dosing and analytical protocols. [b] Dosed at 2 mg/kg. [c] Compounds **9** and **13j** dosed at 30 mg/kg; compounds **13h**, **13i** and **20** dosed at 10 mg/kg.

Table 7. Food-Mix Studies with Compound **20**[a]

	compound distribution			
liver ex vivo inhibition[b]		serum (ng mL^{-1})	liver (ng g^{-1})	fat (ng g^{-1})
95%	day 4, 10 a.m.[a]	1136 ± 180	8132 ± 1075	3622 ± 556
	day 4, 10 p.m.[a]	1086 ± 91	9541 ± 1216	3360 ± 778

[a] See Experimental Section for study protocols. [b] Dosed at 0.5 mg of compound **20** per gram of food.

An interesting trend emerged when comparing the 2-chloro analogues versus the 2-*des*-chloro analogues. The chloro analogue **13j** (Y = Cl) showed 56% ex vivo inhibition in the liver and 54% inhibition in the fat when orally dosed at 10 mg/kg. In contrast, the *des*-chloro analogue **8b** (Y = H) showed marginal liver inhibition even when tested at higher dose (50 mg/kg). Similarly, the chloro analogue **20** showed 80% inhibition at 10 mpk in epididymal fat (Y = Cl), while the *des*-chloro analogue **9** showed only 25% inhibition at the same dose (Y = H). Replacing the 2-Cl group in compound **13j** with a fluoro group (**13k**) had a dramatic effect on the ex vivo potency of this compound. A significant drop in potency both in the liver and fat was observed (< 10% inhibition at 10 mg/kg). The carboxylic acid analogue **13h** and amido analogue **13i** showed good ex vivo inhibition in liver (59 and 56%, respectively) when dosed at 10 mg/kg. Compound **13h** also showed a 40% inhibition in the epididymal fat ex vivo assay.

On the basis of the ex vivo inhibition data, a few compounds were selected for evaluation of pharmacokinetic (PK) properties in C57B6 mice. Compounds were dosed by iv injection (2 mg/kg) and oral administration (10 mg/kg). The results are summarized in Table 6. With the exception of compound **13j**, all of the compounds showed low to moderate clearance and moderate to high oral bioavailability (35−100%).

It is worth mentioning that no direct correlation was observed between plasma AUC values from Table 6 and ex vivo inhibition in liver and fat in Table 5. For instance, of the compounds reported in Table 6, compound **13j** has the lowest plasma AUC but still displayed good ex vivo inhibition both in the liver and fat. In contrast, compound **9** has a high AUC but showed no activity in the ex vivo assay. These results can be rationalized considering the specific tissue distribution of the target. The AUC values reported in Table 6 measure compound levels in the plasma, while 11β-HSD1 is expressed in the liver and adipose tissue. Achieving potent inhibition of 11β-HSD1 in the target tissues is likely to require a balanced profile in terms of potency and pharmacokinetics as well as tissue penetration. A manuscript detailing our findings will be reported in due course.[18]

With a number of compounds demonstrating appropriate in vitro, ex vivo, and PK properties, we decided to perform in vivo proof of concept studies. In this report, we wish to present our preliminary in vitro results for compound **20**.

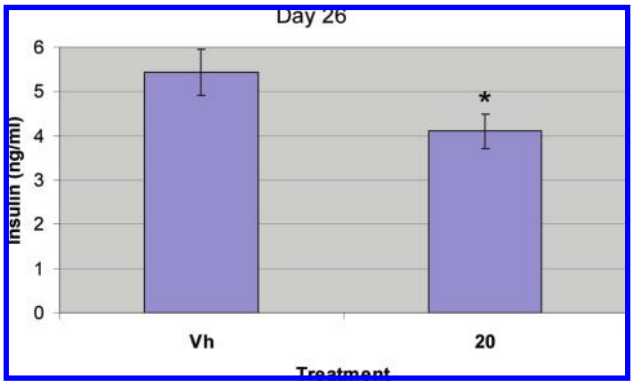

Figure 4. Compound **20** on fasting insulin levels dosed by food mix ($p < 0.05$, see Experimental Section for assay protocols).

Design and Results of the in vivo Studies. The relationship between cortisol and insulin is important to energy balance and can become dysregulated with chronic stress.[19] Cortisol has been shown to directly inhibit insulin secretion from pancreatic β-cells,[20] eventually leading to insulin resistance. We reasoned that administering our compounds using oral gavage for a prolonged period (~28 days) could lead to a significant stress response and impact cortisol levels in animals, ultimately affecting insulin and glucose levels. Therefore, we decided to mix the compound in food in order to minimize handling of the animals. Before we could move forward with the food mix in vivo studies with compound **20**, we confirmed that this compound displays a significant level of ex vivo inhibition when mixed in food. B6-DIO mice (n = 4) were given a high fat diet containing 0.5 mg of compound **20** per g of high fat diet for 96 h. Mice consumed 2.5 g of high fat food and compound mixture per day, indicating that the dose of the compound was 30 mg/kg. All mice were sacrificed, and liver and fat tissues were collected as described in the Experimental Section. Table 7 summarizes the liver ex vivo inhibition using the food mix studies as well as compound levels in liver and fat. Compound **20** showed 95% inhibition after 96 h of dosing. Significant levels of compound **20** were found in target tissues (liver and fat) when measured. On the basis of its favorable ex vivo profile and tissue distribution, compound **20** was advanced to a 28-day food mix study in DIO mice. C57/B6 DIO mice (26 weeks old, 20 weeks on high fat diet, 60% calories from fat) were

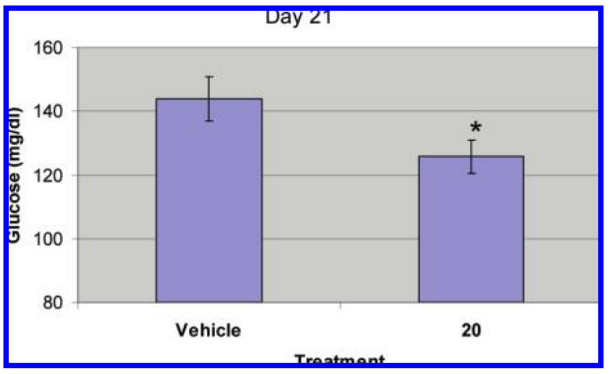

Figure 5. Compound **20** on fed glucose levels dosed by food mix ($p < 0.05$, see Experimental Section for assay protocols).

given a high fat diet containing 0.5 mg of compound per gram of high fat diet for 28 days. As shown in Figures 4 and 5, compound **20** significantly reduced fed glucose as well as fasting insulin levels. No effect was observed on the fasted glucose and the fed insulin. Effects on both food intake and body weight were not observed, and the animals appeared active and healthy with no visible abnormalities.

Conclusion

In summary, we have reported the synthesis and in vitro/in vivo activity of novel potent and selective 2,4-disubsituted benzenesulfonamides. This class of compounds showed good potency against human and mouse 11β-HSD1 and displayed good pharmacokinetics in mice and robust ex vivo inhibition in the liver and fat. To minimize stress response in animals, we administered compound **20** in a high-fat diet food mix. We established that compound **20** achieved high concentrations in target tissues and showed 95% inhibition in the ex vivo assay. A 28-day DIO efficacy study in mice with compound **20** showed a significant reduction in the fed glucose as well as the fasted insulin levels.

Experimental Section

Chemistry. Commercial reagents and solvents were used as received without further purification. Final compounds were either purified by silica gel column chromatography using Merck silica gel 60 (230−400 mesh) or commercially available prepacked silica gel cartridges. Proton nuclear magnetic spectroscopy ^{1}H NMR spectra (400 MHz) were obtained on a Bruker 400 spectrometer. Chemical shifts are reported in parts per million relative to Me_4Si (TMS) as internal standard. Low-resolution mass spectra (MS) were obtained using a micromass platform electrospray ionization quadrapole mass spectrometer. High-resolution exact mass measurements (HRMS) were performed on a Bruker ApexIII 7T FT/ICR/MS with electrospray ionization. Purity of compounds was also analyzed by reverse phase HPLC using the following two conditions: (system A) H_2O/MeCN/0.1% formic acid; (system B) H_2O/MeOH/0.1% formic acid (a gradient of 5−100% B in 7 min followed by 2 min at 100%. A satisfying purity of ≥95% was achieved with both methods.

(3*R*)-1-(4-Fluoro-2-(trifluoromethyl)phenyl)-3-methylpiperazine (5). A mixture of **3** (31.50 g, 315.00 mmol), **4** (72.90 g, 300.00 mmol), BINAP (7.47 g, 12.00 mmol), *t*-BuONa (58.00 g, 600.00 mmol), and $Pd_2(dba)_3$ (5.94 g, 6.00 mmol) was purged with N_2. Anhydrous toluene (1000 mL) was added, and the resulting mixture was purged with N_2 and then heated in an oil bath at 100 °C under N_2 for 5 h. After cooling to rt, the mixture was concentrated and filtered through a pad of celite using Et_2O. The organic layer was concentrated, diluted with Et_2O (500 mL), filtered through a pad of celite, and extracted with 10% aq HCl (2 × 80 mL). The combined aqueous layers were cooled to 0 °C and basified with solid NaOH (to pH ∼ 10) and extracted with Et_2O (3 × 200 mL). The combined organic layers were dried over $MgSO_4$ and concentrated under vacuum to give **5** as a brown oil (82.20 g, 99%). The material was used in subsequent reactions without further purification.

General Procedure A. To a solution of **5** (5.00 g, 19.00 mmol) in CH_2Cl_2 (50 mL) at 0 °C was added diisopropylethylamine (6.62 mL, 38.00 mmol) and phenylsulfonyl chloride **6** (22.80 mmol). After stirring at rt overnight, the reaction mixture washed with saturated aq $NaHCO_3$. The aqueous layer was extracted with CH_2Cl_2 (2 × 50 mL). The organic layers were combined and dried over Na_2SO_4. The crude product was purified on SiO_2 gel column eluted with 5−15% EtOAc in hexanes to give the corresponding benezenesulfonamide **7**.

(2*R*)-1-(4-Bromophenylsulfonyl)-4-(4-fluoro-2-(trifluoromethyl)-phenyl)-2-methylpiperazine (7a). Prepared according to general procedure A, from **5** (1.00 g, 3.80 mmol), 4-bromobenzenesulfonyl chloride (1.07 g, 4.20 mmol) and diisopropylethylamine (1.32 mL, 7.60 mmol), in 88% yield (1.62 g) as a light-yellow solid. ^{1}H NMR (400 MHz, $CDCl_3$) δ ppm 1.20 (d, J = 6.6 Hz, 3 H) 2.64−2.83 (m, 2 H) 2.86−2.95 (m, 1 H) 3.03 (dd, J = 11.0, 3.4 Hz, 1 H) 3.27−3.40 (m, 1 H) 3.71 (d, J = 12.6 Hz, 1 H) 4.22 (dd, J = 6.6, 3.5 Hz, 1 H) 7.16−7.40 (m, 3 H) 7.60−7.76 (m, 4 H). HRMS: calcd for $C_{18}H_{17}BrF_4N_2O_2S$ $[M+H]^+$ 481.0203; found 481.0206.

(2*R*)-4-(4-(4-Fluoro-2-(trifluoromethyl)phenyl)-2-methylpiperazin-1-ylsulfonyl)benzonitrile (7b). Prepared according to general procedure A, using **5** (0.30 g, 1.14 mmol), 4-cyanobenzene-1-sulfonyl chloride (0.23 g, 1.14 mmol), and diisopropylethylamine (0.40 mL, 2.28 mmol). The compound was obtained in 94% yield (457 mg) as an off-white solid. ^{1}H NMR (400 MHz, $CDCl_3$) δ ppm 1.20 (d, J = 6.8 Hz, 3 H), 269−2.83 (m, 2 H), 2.87−2.97 (m, 1 H), 3.03 (dd, J = 11.1, 3.5 Hz, 1 H), 3.37 (td, J = 12.2, 3.2 Hz, 1 H), 3.75 (d, J = 12.9 Hz, 1 H), 4.16−4.31 (m, 1 H), 7.20−7.31 (m, 2 H), 7.34 (dd, J = 8.8, 2.8 Hz, 1 H), 7.84 (d, J = 8.6 Hz, 2 H), 7.96 (d, J = 8.6 Hz, 2 H). HRMS: calcd for $C_{19}H_{17}F_4N_3O_2S$ $[M+H]^+$, 428.1050; found 428.1057.

(2*R*)-4-(4-Fluoro-2-(trifluoromethyl)phenyl)-1-(4-methoxyphenylsulfonyl)-2-methylpiperazine (7c). Prepared according to general procedure A, using **5** (0.20, 0.76 mmol), 4-methoxybenzenesulfonyl chloride (0.19 g, 0.92 mmol), and diisopropylethylamine (0.33 mL, 1.90 mmol). The compound was obtained in 42% yield (136 mg) as a white solid. ^{1}H NMR (400 MHz, DMSO-d_6) δ ppm 1.06 (d, J = 6.6 Hz, 3 H) 2.57−2.76 (m, 2 H) 2.76−2.87 (m, 1 H) 2.96 (d, J = 11.6 Hz, 1 H) 3.05−3.21 (m, 1 H) 3.61 (d, J = 13.1 Hz, 1 H) 3.86 (s, 3 H) 3.98−4.13 (m, 1 H) 7.15 (d, J = 8.6 Hz, 2 H) 7.44−7.62 (m, 3 H) 7.77 (d, J = 8.6 Hz, 2 H). HRMS: calcd for $C_{19}H_{20}F_4N_2O_3S$ $[M+H]^+$, 433.1204; found 433.1204.

(2*R*)-4-(4-Fluoro-2-(trifluoromethyl)phenyl)-2-methyl-1-(4-(trifluoromethoxy)-phenylsulfonyl)-piperazine (7d). Prepared according to general procedure A, using **5** (0.20 g, 0.76 mmol), 4-trifluoromethoxysulfonyl chloride (0.24 g, 0.92 mmol), and diisopropylethylamine (0.33 mL, 1.90 mmol). The compound was obtained in 17% yield (62 mg) as a white solid. ^{1}H NMR (400 MHz, DMSO-d_6) δ ppm 1.09 (d, J = 6.6 Hz, 3 H) 2.64−2.74 (m, 2 H) 2.83 (d, J = 12.1 Hz, 1 H) 2.95 (dd, J = 11.4, 3.5 Hz, 1 H) 3.17−3.26 (m, 1 H) 3.69 (d, J = 12.9 Hz, 1 H) 4.09−4.17 (m, 1 H) 7.49−7.60 (m, 3 H) 7.63 (d, J = 8.6 Hz, 2 H) 8.00 (d, J = 8.8 Hz, 2 H). HRMS: calcd for $C_{19}H_{17}F_7N_2O_3S$ $[M+H]^+$, 487.0921; found 487.0922.

General Procedure B (Buchwald Amination)

(2*R*)-4-[4-Fluoro-2-(trifluoromethyl)phenyl]-2-methyl-1-[(4-piperidin-1-ylphenyl)sulfonyl]piperazine (8a). A mixture of **7a** (0.20 g, 0.42 mmol), piperidine (49 μL, 0.50 mmol), bis-*t*-butylbiphenylphosphine (5.3 mg, 0.042 mmol), *t*-BuONa (121 mg, 1.26 mmol), and $Pd_2(dba)_3$ (19.2 mg, 0.021 mmol) was purged with N_2. Anhydrous toluene (80 mL) was added and purged with N_2 again. The resulting mixture was heated in an oil bath at

110 °C under N_2 for 5 h, cooled to rt, diluted with EtOAc (100 mL), filtered through a pad of celite, and washed with EtOAc (100 mL). The combined organic layer was washed with saturated aqueous $NaHCO_3$. The aqueous layer was extracted with EtOAc (2 × 50 mL). The organic layers were combined and dried over Na_2SO_4. The crude product was purified on SiO_2 gel column eluted with 0−25% MeOH in EtOAc to give **8a** as a light-yellow solid in 48% yield. ^{1}H NMR (400 MHz, $CDCl_3$) δ ppm 1.20 (d, J = 6.8 Hz, 3 H) 1.61−1.77 (m, 6 H) 2.64−2.72 (m, 1 H) 2.73−2.84 (m, 1 H) 2.82−2.90 (m, 1 H) 3.04 (dd, J = 10.9, 3.5 Hz, 1 H) 3.29 (dd, J = 12.6, 3.28 Hz, 1 H) 3.32−3.41 (m, 4 H) 3.65 (d, J = 12.4 Hz, 1 H) 4.14−4.26 (m, 1 H) 6.90 (d, J = 9.1 Hz, 2 H) 7.15−7.24 (m, 1 H) 7.27−7.37 (m, 2 H) 7.65 (d, J = 9.1 Hz, 2 H). HRMS: calcd for $C_{23}H_{27}F_4N_3O_2S$ $[M+H]^+$, 486.1833; found 486.1828.

4-[4-({(2*R*)-4-[4-Fluoro-2-(trifluoromethyl)phenyl]-2-methylpiperazin-1-yl}sulfonyl)phenyl]morpholine (8b). Prepared according to the procedure B, using **7a** (0.20 g, 0.42 mmol) and morpholine (42 μL, 0.50 mmol). The desired product was obtained in 53% yield (108 mg) as a yellow solid. ^{1}H NMR (400 MHz, $CDCl_3$) δ ppm 1.19 (d, J = 6.6 Hz, 3 H) 2.64−2.86 (m, 2 H) 2.88 (s, 1 H) 3.05 (dd, J = 11.0, 3.7 Hz, 1 H) 3.25−3.33 (m, 5 H) 3.59−3.71 (m, J = 12.4 Hz, 1 H) 3.82−3.91 (m, 4 H) 4.09−4.26 (m, 1 H) 6.81−6.96 (m, 2 H) 7.12−7.36 (m, 3 H) 7.58−7.76 (m, 2 H). HRMS: calcd for $C_{22}H_{25}F_4N_3O_3S$ $[M+H]^+$, 488.1626; found 488.1607.

(2*R*)-4-(4-(4-Fluoro-2-(trifluoromethyl)phenyl)-2-methylpiperazin-1-ylsulfonyl)benzamide (9). To compound **7b** (457.0 mg, 1.07 mmol) was added a solution of TMS-CF_3 (0.5 M in THF) (7.49 mL, 3.745 mmol). The mixture was cooled to 0 °C; TBAF (1.0 M in THF, 1.07 mL, 1.07 mmol) was added slowly to the reaction mixture. After stirring at this temperature for 30 min, the reaction mixture was brought to rt, and an additional 7 mL of TMS-CF_3 and TBAF (0.54 mL) were then added. The reaction mixture was heated up to 50 °C, for 3 days. It was then cooled to rt, quenched with saturated aqueous $NaHCO_3$, and extracted with CH_2Cl_2 (2 × 50 mL). The organic layers were combined and washed with brine, dried over Na_2SO_4, and concentrated to give an orange gum, which was purified by preparative HPLC under neutral conditions to afford **9** as a light-tan color solid (151.8 mg) in 25% yield. ^{1}H NMR ($CDCl_3$, 400 MHz): δ ppm 1.19 (d, J = 6.8 Hz, 3 H), 2.63−2.81 (m, 2 H), 2.83−2.96 (m, 1 H), 3.02 (dd, J = 11.2, 3.4 Hz, 1 H), 3.37 (td, J = 12.1, 3.0 Hz, 1 H), 3.75 (d, J = 12.6 Hz, 1 H), 4.25 (d, J = 6.8 Hz, 1 H), 5.74 (br s, 1 H),6.12 (br s, 1 H), 7.17−7.30 (m, 2 H), 7.33 (dd, J = 8.8, 2.8 Hz, 1 H), 7.79−8.10 (m, 4 H). HRMS: calcd for $C_{19}H_{19}F_4N_3O_3S$ $[M+H]^+$, 446.1156; found 446.1156.

(2*R*)-4-[4-Fluoro-2-(trifluoromethyl)phenyl]-2-methyl-1-{[4-(1*H*-tetrazol-5-yl)phenyl]sulfonyl}piperazine (10). The nitrile **7b** (150 mg, 0.35 mmol), NaN_3 (66.0 mg, 1.05 mmol), and triethylamine hydrochloride (139.0 mg, 1.05 mmol) were dissolved in toluene (3.50 mL). The mixture was heated at 100 °C for 16 h, after which the reaction was judged complete by LCMS. The reaction mixture was then diluted with H_2O (100 mL) and extracted into EtOAc (3 × 25 mL). The combined organic layers were washed with 5% HCl, dried over $MgSO_4$, filtered, and then concentrated under vacuum. The residue was purified via trituration with ether/hexanes, affording the desired compound as a white powder (97.0 mg) in 61% yield. ^{1}H NMR (400 MHz, $CDCl_3$) δ ppm 1.22 (d, J = 6.6 Hz, 3 H) 2.67−2.86 (m, 2 H) 2.88−2.97 (m, 1 H) 3.04 (dd, J = 11.1, 3.3 Hz, 1 H) 3.34−3.48 (m, 1 H) 3.78 (d, J = 12.6 Hz, 1 H) 4.13−4.36 (m, 1 H) 7.13−7.39 (m, 3 H) 8.00 (d, J = 8.3 Hz, 2 H) 8.33 (d, J = 8.3 Hz, 2 H). HRMS: calcd for $C_{19}H_{18}F_4N_6O_2S$ $[M+H]^+$, 471.1221; found 471.1225.

(2*R*)-1-(4-Bromo-2-chlorophenylsulfonyl)-4-(4-fluoro-2-(trifluoromethyl)phenyl)-2-methylpiperazine (12a). Prepared according to general procedure A, using **5** (3.26 g, 12.45 mmol), 4-bromo-2-chlorobenzene-1-sulfonyl chloride (3.18 g, 10.96 mmol), and diisopropylethylamine (5.42 mL, 31.12 mmol). The compound was obtained as a white solid (5.72 g) in 97% yield. ^{1}H NMR (400 MHz, $CDCl_3$) δ ppm 1.35 (d, J = 6.8 Hz, 3 H) 2.65−2.83 (m, 2 H) 2.84−2.95 (m, 1 H) 3.07 (dd, J = 11.1, 3.5 Hz, 1 H) 3.45−3.62 (m, 1 H) 3.64−3.81 (m, 1 H) 4.04−4.17 (m, 1 H) 7.12−7.26 (m, 1 H) 7.29−7.42 (m, 2 H) 7.54 (dd, J = 8.5, 1.9 Hz, 1 H) 7.72 (d, J = 1.8 Hz, 1 H) 7.99 (d, J = 8.6 Hz, 1 H). HRMS: calcd for $C_{18}H_{16}BrClF_4N_2O_2S$ $[M+H]^+$, 514.9813; found 514.9815.

(2*R*)-1-(4-Bromo-2-fluorophenylsulfonyl)-4-(4-fluoro-2-(trifluoromethyl)phenyl)-2-methylpiperazine (12b). Prepared according to general procedure A, using **5** (1.00 g, 3.80 mmol), 2-fluoro-4-bromobenzenesulfonyl chloride (1.30 g, 4.60 mmol), and diisopropylethylamine (1.70 mL, 9.50 mmol). The compound was obtained in 84% yield (1.60 g) as a light-yellow solid. ^{1}H NMR (400 MHz, DMSO-d_6) δ ppm 1.11 (d, J = 6.6 Hz, 3 H) 2.65−2.87 (m, 2 H) 2.90−3.09 (m, 2 H) 3.21−3.31 (m, 1 H) 3.75 (d, J = 12.9 Hz, 1 H) 4.13−4.28 (m, 1 H) 7.37−7.61 (m, 1 H) 8.00−8.29 (m, 5 H). HRMS: calcd for $C_{18}H_{16}BrF_5N_2O_2S$ $[M + H]^+$, 499.0109; found 499.0109.

(2*R*)-*N*-[3-Chloro-4-({4-[4-fluoro-2-(trifluoromethyl)phenyl]-piperazin-1-yl}sulfonyl)phenyl]morpholine-4-carboxamide (12c). Synthesized according to the general procedure A, using **5** (100.0 mg, 0.40 mmol), diisopropylethylamine (0.14 mL, 0.80 mmol), and 2-chloro-4-[(morpholine-4-carbonyl)-amino]-benzenesulfonyl chloride (136.6 mg, 0.40 mmol) in CH_2Cl_2 (1.5 mL). The compound was obtained in 88% yield as a white solid. ^{1}H NMR (400 MHz, $CDCl_3$) δ ppm 1.35 (d, J = 6.8 Hz, 3 H) 2.61−2.81 (m, 2 H) 2.88 (d, J = 11.6 Hz, 1 H) 3.06 (dd, J = 11.1, 3.5 Hz, 1 H) 3.46−3.60 (m, 5 H) 3.66 (d, J = 13.1 Hz, 1 H) 3.70−3.81 (m, 4 H) 4.09 (dd, J = 12.2, 7.20 Hz, 1 H) 6.64 (s, 1 H) 7.14−7.24 (m, 1 H) 7.27−7.38 (m, 3 H) 7.75 (d, J = 2.0 Hz, 1 H) 7.99 (d, J = 8.8 Hz, 1 H). HRMS: calcd for $C_{23}H_{25}ClF_4N_4O_4S$ $[M+H]^+$, 565.1294; found 565.1304.

(2*R*)-3-Chloro-4-(4-(4-fluoro-2-(trifluoromethyl)phenyl)-2-methylpiperazin-1-ylsulfonyl)-*N*,*N*-dimethylaniline (13a). Prepared according to the general procedure B, using **12a** (500.0 mg, 1.01 mmol), 2.0 M *N*,*N*-dimethylamine (550.0 μL, 1.10 mmol), $Pd_2(dba)_3$ (27.0 mg, 0.03 mmol), BINAP (38.0 mg, 0.06 mmol), and *t*-BuONa (144.0 mg, 1.50 mmol). The compound was obtained as a white solid (180.0 mg) in 39% yield. ^{1}H NMR (400 MHz, $CDCl_3$) δ ppm 1.34 (d, J = 6.8 Hz, 3 H) 2.64−2.83 (m, 2 H) 2.82−2.91 (m, 1 H) 3.05 (s, 6 H) 3.09 (dd, J = 11.0, 3.4 Hz, 1 H) 3.40−3.58 (m, 1 H) 3.59−3.72 (m, 1 H) 3.9−4.18 (m, J = 3.3 Hz, 1 H) 6.53 (dd, J = 9.0, 2.7 Hz, 1 H) 6.72 (d, J = 2.8 Hz, 1 H) 7.08−7.23 (m, 1 H) 7.29−7.43 (m, 2 H) 7.91 (d, J = 9.1 Hz, 1 H). HRMS: calcd for $C_{20}H_{22}ClF_4N_3O_2S$ $[M+H]^+$, 480.1130; found 480.1129.

(2*R*)-1-[(2-Chloro-4-pyrrolidin-1-ylphenyl)sulfonyl]-4-[4-fluoro-2-(trifluoromethyl)phenyl]-2-methylpiperazine (13b). Prepared according to the general procedure B, using **12a** (500.0 mg, 1.00 mmol) and pyrrolidine (92.8 μL, 1.10 mmol), $Pd_2(dba)_3$ (27.0 mg, 0.03 mmol), BINAP (38.0 mg, 0.06 mmol), and *t*-BuONa (144.0 mg, 1.50 mmol). The compound was obtained as a white solid (136.0 mg), in 27% yield. ^{1}H NMR (400 MHz, $CDCl_3$) δ ppm 1.36 (d, J = 6.8 Hz, 3 H) 1.41 (s, 9 H) 2.63−2.83 (m, 2 H) 2.81−2.92 (m, 1 H) 3.09 (dd, J = 11.0, 3.4 Hz, 1 H) 3.42−3.57 (m, 1 H) 3.58−3.68 (m, 1 H) 4.05−4.17 (m, 1 H) 4.18−4.30 (m, 1 H) 6.52 (dd, J = 8.8, 2.3 Hz, 1 H) 6.72 (d, J = 2.5 Hz, 1 H) 7.14−7.25 (m, 1 H) 7.29−7.41 (m, 2 H) 7.82 (d, J = 8.8 Hz, 1 H). HRMS: calcd for $C_{22}H_{24}ClF_4N_3O_2S$ $[M+H]^+$, 506.1287; found 506.1285

(2*R*)-1-[(2-Chloro-4-piperidin-1-ylphenyl)sulfonyl]-4-[4-fluoro-2-(trifluoromethyl)phenyl]-2-methylpiperazine (13c). Prepared according general procedure B, using **12a** (250.0 mg, 0.49 mmol), piperidine (52.5 μL, 0.53 mmol), $Pd_2(dba)_3$ (25.0 mg, 0.03 mmol), BINAP (31.0 mg, 0.06 mmol), and *t*-BuONa (77.0 mg, 0.74 mmol). The compound was obatined as a white solid (125.0 mg), in 43% yield. ^{1}H NMR (400 MHz, DMSO-d_6) δ ppm 1.18−1.27 (m, 3 H) 1.47−1.69 (m, 6 H) 2.63−2.75 (m, 2 H) 2.76−2.91 (m, 1 H) 2.90−3.08 (m, 1 H) 3.21−3.33 (m, 1 H) 3.34−3.42 (m, J = 5.8 Hz, 4 H) 3.46−3.60 (m, 1 H) 3.89−4.05 (m, 1 H) 6.94 (dd, J = 9.1, 2.5 Hz, 1 H) 7.02−7.11 (m, J = 2.8 Hz, 1 H) 7.45−7.65 (m, 3 H) 7.75 (d, J = 8.8 Hz, 1 H). HRMS: calcd for $C_{23}H_{26}ClF_4N_3O_2S$ $[M+H]^+$, 520.1443; found 520.1445.

(2*R*)-1-{[2-Chloro-4-(4-fluoropiperidin-1-yl)phenyl]sulfonyl}-4-[4-fluoro-2-(trifluoromethyl)phenyl]-2-methylpiperazine (13d). Prepared according to the general procedure B, using **12a** (400.0 mg, 0.83 mmol), 4-fluoropiperidine hydrochloride (139.5 mg, 1.00 mmol), $Pd_2(dba)_3$ (37.0 mg, 0.04 mmol), BINAP (50.0 mg, 0.08 mmol), and *t*-BuONa (200.0 mg, 2.08 mmol). The compound was obtained as a white solid (10.0 mg), in 3% yield. ^{1}H NMR (400 MHz, DMSO-d_6) δ ppm 1.06−1.31 (m, 7 H) 2.61−2.76 (m, 2 H) 2.75−2.88 (m, 1 H) 2.90−3.07 (m, 1 H) 3.35−3.46 (m, 5 H) 3.46−3.67 (m, 1 H) 3.93−4.05 (m, J = 7.3 Hz, 1 H) 4.73−5.01 (m, 1 H) 6.92−7.03 (m, 2 H) 7.17 (d, J = 2.8 Hz, 2 H) 7.78 (d, J = 9.6 Hz, 2 H).

(2*R*)-1-{[2-Chloro-4-(4,4-difluoropiperidin-1-yl)phenyl]sulfonyl}-4-[4-fluoro-2-(trifluoromethyl)phenyl]-2-methylpiperazine (13e). Prepared according to the general procedure B, using **12a** (400.0 mg, 0.83 mmol), 4,4-difluoropiperidine hydrochloride (157.5 mg, 1.00 mmol), $Pd_2(dba)_3$ (37.0 mg, 0.04 mmol), BINAP (50.0 mg, 0.08 mmol), and *t*-BuONa (200.0 mg, 2.08 mmol). The compound was obtained as a white solid (35.0 mg), in 8% yield. ^{1}H NMR (400 MHz, $CDCl_3$) δ ppm 1.34 (d, J = 6.8 Hz, 3 H) 1.96−2.17 (m, 4 H) 2.65−2.84 (m, 2 H) 2.85−2.94 (m, 1 H) 3.09 (dd, J = 10.9, 3.8 Hz, 1 H) 3.41−3.59 (m, 5 H) 3.67 (d, J = 13.1 Hz, 1 H) 4.00−4.20 (m, 1 H) 6.78 (dd, J = 9.0, 2.7 Hz, 1 H) 6.96 (d, J = 2.5 Hz, 1 H) 7.15−7.25 (m, 1 H) 7.95 (d, J = 9.1 Hz, 1 H).

(2*R*)-1-[3-Chloro-4-({(2*R*)-4-[4-fluoro-2-(trifluoromethyl)phenyl]-2-methylpiperazin-1-yl}sulfonyl)phenyl]-*N*,*N*-dimethylpiperidin-4-amine (13f). Prepared according to the general procedure B, using **12a** (250.0 mg, 0.50 mmol), 4-dimethylaminopiperadine (77.0 mg, 0.60 mmol), $Pd_2(dba)_3$ (23.0 mg, 0.02 mmol), BINAP (31.0 mg, 0.05 mmol), and *t*-BuONa (72.0 mg, 0.08 mmol). The compound was obtained as a yellow solid (92.0 mg), in 33% yield. ^{1}H NMR (400 MHz, $CDCl_3$) δ ppm 1.34 (d, J = 6.8 Hz, 3 H) 1.53−1.70 (m, 1 H) 1.89−2.05 (m, 2 H) 2.38 (s, 6 H) 2.66−2.82 (m, 3 H) 2.83−2.99 (m, 3 H) 3.03−3.14 (m, 1 H) 3.31−3.43 (m, 1 H) 3.42−3.58 (m, 1 H) 3.66 (d, J = 13.1 Hz, 1 H) 3.89 (d, J = 13.4 Hz, 2 H) 4.02−4.17 (m, 1 H) 6.74 (dd, J = 9.0, 2.7 Hz, 1 H) 6.92 (d, J = 2.8 Hz, 1 H) 7.12−7.25 (m, 1 H) 7.33 (dd, J = 8.8, 3.3 Hz, 2 H) 7.91 (d, J = 8.8 Hz, 1 H). HRMS: calcd for $C_{25}H_{31}ClF_4N_4O_2S$ $[M+H]^+$, 563.1865; found 563.1886.

(2*R*)-1-(3-Chloro-4-(2-fluoro-4-(4-fluoro-2-(trifluoromethyl)-phenyl)piperazin-1-ylsulfonyl)phenyl)piperidin-4-ol (13g). Prepared according to the general procedure B, from the bromide precursor (500 mg, 1.0 mmol), 4-hydroxy-piperadine (98 mg, 0.6 mmol), $Pd_2(dba)_3$ (45 mg, 0.05 mmol), BINAP (62 mg, 0.10 mmol), and *t*-BuONa (140 mg, 1.45 mmol). The compound was obtained as a yellow solid (77 mg), in 16% yield. ^{1}H NMR (400 MHz, DMSO-d_6) δ 1.22 (d, J = 6.6 Hz, 3H), 1.34−1.46 (m, 2H), 1.73−1.84 (m, 2H), 2.64−2.75 (m, 2H), 2.83 (d, J = 12.4 Hz, 1H), 2.98 (dd, J = 3.4, 11.0 Hz, 1H), 3.04−3.15 (m, 2H), 3.95−4.01 (m, 1H), 3.53 (d, J = 12.9 Hz, 1H), 3.68−3.78 (m, 3H), 4.75 (d, J = 4.0 Hz, 1H), 6.95 (dd, J = 2.5, 9.1 Hz, 1H), 7.11 (d, J = 2.5 Hz, 1H), 7.47−7.66 (m, 3H), 7.76 (d, J = 8.8 Hz, 1H). HRMS: calcd for $C_{24}H_{26}ClF_4N_3O_4S$ $[M + H]^+$, 564.1341; found 564.1342.

(2*R*)-1-(3-Chloro-4-(4-(4-fluoro-2-(trifluoromethyl)phenyl)-2-methylpiperazin-1-ylsulfonyl)phenyl)piperidine-4-carboxylic Acid (13h). Prepared according to the general procedure B, from **12a** (1.00 g, 1.95 mmol), ethyl piperidine-4-carboxylate (360.0 μL, 2.34 mmol), $Pd_2(dba)_3$ (92.0 mg, 0.10 mmol), BINAP (125.0 mg, 0.20 mmol), and *t*-BuONa (282.0 mg, 2.93 mmol). The product was purified by silica gel column chromatography, then hydrolyzed by using KOH (10.00 mmol) in a 2:1 mixture (v/v) of MeOH/THF (6 mL) at rt for 5 h. It was diluted with water (10 mL) and acidified with 10% aq HCl to pH around 3. The precipitate was collected by filtration and washed with water to afford the desired product as a white solid (245.0 mg) in 21% overall yield. ^{1}H NMR (400 MHz, $CDCl_3$) δ ppm 1.34 (d, J = 6.8 Hz, 3 H) 1.76−1.93 (m, 2 H) 2.07 (dd, J = 13.4, 3.8 Hz, 2 H) 2.54−2.67 (m, 1 H) 2.68−2.82 (m, 2 H) 2.81−2.93 (m, 1 H) 2.95−3.12 (m, 3 H) 3.35−3.58 (m, 1 H) 3.60−3.68 (m, 1 H) 3.75−3.86 (m, 2 H) 4.03−4.17 (m, 1 H) 6.75 (dd, J = 9.1, 2.5 Hz, 1 H) 6.93 (d, J = 2.5 Hz, 1 H) 7.13−7.25 (m, 1 H) 7.29−7.38 (m, 2 H) 7.92 (d, J = 9.1 Hz, 1 H). HRMS: calcd for $C_{24}H_{26}ClF_4N_3O_4S$ $[M + H]^+$, 564.1341; found 564.1368.

(2*R*)-1-(3-Chloro-4-(4-(4-fluoro-2-(trifluoromethyl)phenyl)-2-methylpiperazin-1-ylsulfonyl)phenyl)piperidine-4-carboxamide (13i). Prepared according to the general procedure B, using **12a** (1.00 g, 1.95 mmol), piperidine-4-carboxamide (299.0 mg, 2.34 mmol), $Pd_2(dba)_3$ (92.0 mg, 0.10 mmol), BINAP (125.0 mg, 0.20 mmol), and *t*-BuONa (282.0 mg, 2.93 mmol). The compound was obtained as a white solid (210.0 mg) in 19% yield. ^{1}H NMR (400 MHz, $CDCl_3$) δ ppm 1.36 (d, J = 6.8 Hz, 3 H) 1.73−1.90 (m, 2 H) 1.93−2.05 (m, 2 H) 2.33−2.48 (m, 1 H) 2.64−2.84 (m, 3 H) 2.85−3.00 (m, 3 H) 3.09 (dd, J = 10.9, 3.3 Hz, 1 H) 3.45−3.57 (m, 1 H) 3.61−3.73 (m, 1 H) 3.88 (d, J = 13.1 Hz, 2 H) 4.03−4.21 (m, 1 H) 5.40 (br s, 1 H) 5.53 (br s, 1 H) 6.74 (dd, J = 9.1, 2.5 Hz, 1 H) 6.92 (d, J = 2.5 Hz, 1 H) 7.15−7.26 (m, 1 H) 7.29−7.40 (m, 2 H) 7.92 (d, J = 9.1 Hz, 1 H). HRMS: calcd for $C_{24}H_{27}ClF_4N_4O_3S$ $[M+H]^+$, 563.1501; found 563.1509.

(2*R*)-4-[3-Chloro-4-({(2*R*)-4-[4-fluoro-2-(trifluoromethyl)phenyl]-2-methylpiperazin-1-yl}sulfonyl)phenyl]morpholine (13j). Prepared according to the general procedure B, from **12a** (7.0 g, 13.8 mmol), morpholine (1.10 mL, 15.10 mmol), $Pd_2(dba)_3$ (382.0 mg, 0.42 mmol), BINAP (615 mg, 1.43 mmol), and *t*-BuONa (2.00 g, 4.68 mmol) and recrystallized as white needles (3.90 g) in 58% yield. ^{1}H NMR (400 MHz, $CDCl_3$) δ ppm 1.34 (d, J = 6.8 Hz, 3 H) 2.69−2.83 (m, 2 H) 2.84−2.96 (m, 1 H) 3.09 (dd, J = 11.0, 3.4 Hz, 1 H) 3.22−3.39 (m, 4 H) 3.41−3.60 (m, 1 H) 3.67 (d, J = 13.1 Hz, 1 H) 3.79−3.91 (m, 4 H) 4.03−4.20 (m, J = 3.3 Hz, 1 H) 6.75 (dd, J = 9.1, 2.5 Hz, 1 H) 6.93 (d, J = 2.5 Hz, 1 H) 7.14−7.26 (m, 1 H) 7.27−7.38 (m, 2 H) 7.96 (d, J = 9.1 Hz, 1 H). HRMS: calcd for $C_{22}H_{24}ClF_4N_3O_3S$ $[M + H]^+$, 522.1236; found 522.1220.

(2*R*)-4-(3-Fluoro-4-(4-(4-fluoro-2-(trifluoromethyl)phenyl)-2-methylpiperazin-1-ylsulfonyl)phenyl)morpholine (13k). Prepared according general procedure B, from **12b** (200 mg, 0.44 mmol), morpholine (46.0 μL, 53.00 mmol), $Pd_2(dba)_3$ (22.0 mg, 0.02 mmol), BINAP (31.0 mg, 0.05 mmol), and *t*-BuONa (63.0 mg, 0.66 mmol). The compound was obtained a white solid (100.0 mg) in 52% yield. ^{1}H NMR (400 MHz, $CDCl_3$) δ ppm 1.25 (d, J = 6.8 Hz, 3 H) 2.67−2.84 (m, 2 H) 2.89 (s, 1 H) 3.04 (dd, J = 11.1, 3.3 Hz, 1 H) 3.19−3.35 (m, 4 H) 3.36−3.51 (m, 1 H) 3.38−3.47 (m, 1 H) 3.76 (s, 1 H) 3.80−3.93 (m, 4 H) 4.08−4.25 (m, 1 H) 6.53−6.67 (m, 2 H) 7.12−7.25 (m, 1 H) 7.29−7.42 (m, 2 H) 7.73 (t, J = 8.7 Hz, 1 H). HRMS: calcd for $C_{22}H_{24}F_5N_3O_3S$ $[M+H]^+$, 506.1531; found 506.1532.

(2*R*)-4-[3-Chloro-4-({(2*R*)-4-[4-fluoro-2-(trifluoromethyl)phenyl]-2-methylpiperazin-1-yl}sulfonyl)phenyl]-*cis*-2,6-dimethylmorpholine (13l). Prepared according to the general procedure B, using **12a** (250 mg, 0.5 mmol), *cis*-2,6-dimethylmorpholine (69.0 mg, 0.60 mmol), $Pd_2(dba)_3$ (72.0 mg, 0.025 mmol), BINAP (31.0 mg, 0.05 mmol), and *t*-BuONa (72.0 mg, 0.75 mmol). The compound was obtained as a yellow solid (309.0 mg) in 56% yield. ^{1}H NMR (400 MHz, $CDCl_3$) δ ppm 1.28 (d, J = 6.3 Hz, 6 H) 1.34 (d, J = 6.8 Hz, 3 H) 2.56 (dd, J = 12.1, 10.9 Hz, 2 H) 2.66−2.81 (m, 2 H) 2.87 (d, J = 1.0 Hz, 1 H) 3.08 (dd, J = 10.9, 3.5 Hz, 1 H) 3.42−3.60 (m, 3 H) 3.63−3.72 (m, 1 H) 3.71−3.81 (m, 2 H) 3.98−4.21 (m, 1 H) 6.74 (dd, J = 9.1, 2.5 Hz, 1 H) 6.92 (d, J = 2.5 Hz, 1 H) 7.10−7.26 (m, 1 H) 7.28−7.38 (m, 2 H) 7.94 (d, J = 9.1 Hz, 1 H). HRMS: calcd for $C_{24}H_{28}ClF_4N_3O_3S$ $[M+H]^+$, 550.1549; found 550.1550.

(2*R*)-1-{[2-Chloro-4-(4-methylpiperazin-1-yl)phenyl]sulfonyl}-4-[4-fluoro-2-(trifluoromethyl)phenyl]-2-methylpiperazine (13m). Prepared according to the general procedure B, using **12a** (257.0 mg, 0.50 mmol), *N*-methylpiperazine (59 μL, 0.53 mmol), $Pd_2(dba)_3$ (72.0 mg, 0.02 mmol), BINAP (31.0 mg, 0.05 mmol), and *t*-BuONa (72.0 mg, 0.75 mmol). The compound was purified via reversed phase HPLC, using a 10−90% acetonitrile/H_2O gradient and isolated as a white solid (97 mg) in 37% yield. ^{1}H NMR (400 MHz,

$CDCl_3$) δ ppm 1.34 (d, J = 6.8 Hz, 3 H) 2.47 (s, 3 H) 2.65−2.82 (m, 6 H) 2.87 (d, 1 H) 3.08 (d, J = 11.4 Hz, 1 H) 3.38−3.48 (m, 4 H) 3.48−3.59 (m, 1 H) 3.66 (d, J = 13.1 Hz, 1 H) 3.98−4.19 (m, 1 H) 6.76 (dd, J = 9.1, 2.5 Hz, 1 H) 6.94 (d, J = 2.5 Hz, 1 H) 7.15−7.25 (m, 1 H) 7.30−7.39 (m, 2 H) 7.95 (d, J = 9.1 Hz, 1 H). HRMS: calcd for $C_{23}H_{27}ClF_4N_4O_2S$ $[M+H]^+$, 535.1552; found 535.1576.

(2*R*)-1-({2-Chloro-4-[(3*S*)-3-methylpiperazin-1-yl]phenyl}sulfonyl)-4-[4-fluoro-2-(trifluoromethyl)phenyl]-2-methylpiperazine (13n). Prepared according to the general procedure B, using **12a** (257.0 mg, 0.5 mmol), 2-(*S*)-methylpiperazine (60.0 mg, 0.60 mmol), $Pd_2(dba)_3$ (72.0 mg, 0.025 mmol), BINAP (31.0 mg, 0.05 mmol), and *t*-BuONa (72.0 mg, 0.75 mmol). The compound was isolated as a yellow solid in 51% yield. ^{1}H NMR (400 MHz, $CDCl_3$) δ ppm 1.34 (d, J = 6.8 Hz, 3 H) 1.43 (d, J = 6.1 Hz, 3 H) 2.66−2.81 (m, 2 H) 2.84−3.01 (m, 2 H) 3.09 (d, J = 10.9 Hz, 2 H) 3.16−3.31 (m, 2 H) 3.36 (d, J = 2.3 Hz, 1 H) 3.53 (d, J = 11.9 Hz, 2 H) 3.70 (d, J = 3.1 Hz, 2 H) 4.05−4.16 (m, 1 H) 6.77 (dd, J = 9.0, 2.4 Hz, 1 H) 6.86−6.99 (m, 1 H) 7.17−7.23 (m, 1 H) 7.30−7.40 (m, 2 H) 7.86−8.00 (m, 1 H).

(2*R*)-4-[3-Chloro-4-({(2*R*)-4-[4-fluoro-2-(trifluoromethyl)phenyl]-2-methylpiperazin-1-yl}sulfonyl)phenyl]thiomorpholine-1,1-dioxide (13o). Prepared according to the general procedure B, using **12a** (257.0 mg, 0.50 mmol), thiomorpholine-1,1-dioxide (85.0 mg, 0.60 mmol), $Pd_2(dba)_3$ (72 mg, 0.025 mmol), BINAP (31.0 mg, 0.05 mmol), and *t*-BuONa (72.0 mg, 0.75 mmol). The compound was isolated as a pale-yellow solid (51.0 mg), in 18% yield. ^{1}H NMR (400 MHz, $CDCl_3$) δ ppm 1.36 (d, J = 6.8 Hz, 3 H) 2.68−2.84 (m, 2 H) 2.84−2.96 (m, 1 H) 3.01−3.19 (m, 5 H) 3.41−3.59 (m, 1 H) 3.63−3.75 (m, 1 H) 3.91−4.03 (m, 4 H) 4.05−4.22 (m, 1 H) 6.79 (dd, J = 9.0, 2.6 Hz, 1 H) 6.96 (d, J = 2.8 Hz, 1 H) 7.11−7.24 (m, 1 H) 7.29−7.37 (m, 2 H) 8.01 (d, J = 8.8 Hz, 1 H). HRMS: calcd for $C_{22}H_{24}ClF_4N_3O_4S_2$ $[M+H]^+$, 570.0906; found 570.0918.

(2*R*)-4-[3-Chloro-4-({(2*R*)-4-[4-fluoro-2-(trifluoromethyl)phenyl]-2-methylpiperazin-1-yl}sulfonyl)phenyl]piperazin-2-one (13p). Prepared according to the general procedure B, using **12a** (257.0 mg, 0.50 mmol), piperazine-2-one (69.0 mg, 0.60 mmol), $Pd_2(dba)_3$ (72.0 mg, 0.025 mmol), BINAP (31.0 mg, 0.05 mmol), and *t*-BuONa (72.0 mg, 0.75 mmol). The compound was isolated as an off-white solid (50.0 mg), in 19% yield. ^{1}H NMR (400 MHz, DMSO-d_6) δ ppm 1.22 (d, J = 6.6 Hz, 3 H) 2.68 (s, 2 H) 2.77−2.86 (m, 1 H) 2.91−3.03 (m, 1 H) 3.24−3.41 (m, 3 H) 3.47−3.63 (m, 3 H) 3.91 (s, 2 H) 3.99−4.07 (m, 1 H) 6.93 (d, J = 8.8 Hz, 1 H) 7.09 (d, J = 2.5 Hz, 1 H) 7.49−7.64 (m, 3 H) 7.81 (d, J = 9.1 Hz, 1 H) 8.22 (s, 1 H). HRMS: calcd for $C_{22}H_{23}ClF_4N_4O_3S$ $[M+H]^+$ 535.1188; found 535.1195.

(2*R*)-1-(4-*tert*-Butoxy-2-chlorophenylsulfonyl)-4-(4-fluoro-2-(trifluoromethyl)phenyl)-2-methylpiperazine (14a). Prepared according to the general procedure B, using **12a** (514.0 mg, 1.0 mmol), $Pd_2(dba)_3$ (45.0 mg, 0.05 mmol), BINAP (63.0 mg, 0.10 mmol), and *t*-BuONa (192.0 mg, 2.00 mmol), affording the desired product as a white solid (375.0 mg) in an overall 75% yield. ^{1}H NMR (400 MHz, $CDCl_3$) δ ppm 1.34 (d, J = 6.8 Hz, 3 H) 1.44 (s, 9 H) 2.69−2.83 (m, 2 H) 2.88 (s, 1 H) 3.01−3.13 (m, 1 H) 3.48−3.62 (m, 1 H) 3.70 (d, J = 12.9 Hz, 1 H) 4.01−4.20 (m, 1 H) 6.95 (d, J = 8.8 Hz, 1 H) 7.13 (s, 1 H) 7.17−7.24 (m, 1 H) 7.29−7.38 (m, 2 H) 8.01 (d, J = 8.6 Hz, 1 H).

(2*R*)-1-[3-Chloro-4-({(2*R*)-4-[4-fluoro-2-(trifluoromethyl)phenyl]-2-methylpiperazin-1-yl}sulfonyl)phenyl]piperazin-2-one (15a). A mixture of **12a** (257.0 mg, 0.49 mmol), *tert*-butyl 3-oxopiperazine-1-carboxylate (116.0 mg, 0.58 mmol), CuI (5.0 mg, 0.025 mmol), K_3PO_4 (208.0 mg, 0.98 mmol) and *trans*-*N*,*N*′-dimethylcyclohexane-1,2-diamine (14.0 mg, 0.1 0 mmol) was heated in diglyme (1.0 mL) at 165 °C under microwave conditions for 2 h, after which the reaction was judged complete by LCMS. The mixture was diluted with ethyl acetate and washed with saturated sodium bicarbonate solution, dried over Na_2SO_4, decanted, and concentrated in vacuo. The residue was purified via silica gel column chromatography (20−80% ethyl acetate/hexanes), affording the desired compound, (*R*)-*tert*-butyl 4-(3-chloro-4-(4-(4-fluoro-2-(trifluoromethyl)phenyl)-2-methylpiperazin-1-ylsulfonyl)phenyl)-3-oxopiperazine-1-carboxylate, as a white solid (70.0 mg) in 22% yield. ^{1}H NMR (400 MHz, DMSO-d_6) δ ppm 1.25 (d, J = 6.8 Hz, 3 H) 2.65−2.77 (m, J = 8.7 Hz, 2 H) 2.79−2.88 (m, 1 H) 2.93−3.07 (m, 1 H) 3.34−3.45 (m, 1 H) 3.55−3.75 (m, 3 H) 3.78−3.89 (m, J = 6.1 Hz, 2 H) 4.06−4.17 (m, 3 H) 7.42−7.70 (m, 4 H) 7.83 (d, J = 2.3 Hz, 1 H) 8.07 (d, J = 8.6 Hz, 1 H).

A solution of (*R*)-*tert*-butyl 4-(3-chloro-4-(4-(4-fluoro-2-(trifluoromethyl)phenyl)-2-methylpiperazin-1-ylsulfonyl)phenyl)-3-oxopiperazine-1-carboxylate (50.0 mg, 0.08 mmol) was dissolved in CH_2Cl_2 (10.0 mL). Trifluoroacetic acid (2.0 mL) was then added dropwise at ambient temperature, and the reaction mixture was allowed to stir for 5 h, after which it was judged complete by TLC. The reaction mixture was concentrated under vacuum and the residue was dissolved in MeOH/H_2O (∼10 mL 1:10 v/v). Aqueous 1 N NaOH was then added dropwise until the desired product was precipitated. The slurry was filtered and the solid was rinsed with water, affording the desired compound as a white powder in 94% yield. ^{1}H NMR (400 MHz, $CDCl_3$) δ ppm 1.40 (d, J = 6.6 Hz, 3 H) 2.66−2.82 (m, 2 H) 2.87−2.95 (m, 1 H) 3.08 (dd, J = 11.2, 3.4 Hz, 1 H) 3.20−3.31 (m, 3 H) 3.44−3.61 (m, 1 H) 3.61−3.72 (m, 1 H) 3.70−3.81 (m, 4 H) 4.04−4.21 (m, 1 H) 7.13−7.26 (m, 1 H) 7.29−7.37 (m, 2 H) 7.41 (dd, J = 8.6, 2.3 Hz, 1 H) 7.63 (d, J = 2.0 Hz, 1 H) 8.14 (d, J = 8.6 Hz, 1 H). HRMS: calcd for $C_{22}H_{23}ClF_4N_4O_3S$ $[M+H]^+$, 535.1188; found 535.1195.

(2*R*)-1-{[2-Chloro-4-(1*H*-1,2,4-triazol-1-yl)phenyl]sulfonyl}-4-[4-fluoro-2-(trifluoromethyl)phenyl]-2-methylpiperazine (15b). A solution of **12a** (900.0 mg, 2.00 mmol), 1,2,4-triazole (138.0 mg, 2.00 mmol), K_2CO_3 (550.0 mg, 4.00 mmol), and CuI (38.0 mg, 0.20 mmol) in NMP (20.0 mL) was heated under microwave conditions for 30 min at 150 °C, after which the reaction was judged complete by LCMS. The reaction mixture was diluted with EtOAc and washed with saturated aqueous $NaHCO_3$. The organic layer was dried over Na_2SO_4, decanted, and concentrated under vacuum. The resulting residue was purified via reversed phase Gilson HPLC, using a 40−100% ACN/H_2O gradient in the presence of 0.1% formic acid, affording the desired product (603.0 mg) as a white powder in 70% yield. ^{1}H NMR (400 MHz, $CDCl_3$) δ ppm 1.37 (d, J = 6.8 Hz, 3 H) 2.60−2.84 (m, 2 H) 2.93 (d, J = 9.9 Hz, 1 H) 3.09 (dd, J = 11.1, 3.5 Hz, 1 H) 3.42−3.66 (m, 1 H) 3.75 (d, J = 13.4 Hz, 1 H) 4.11−4.23 (m, 1 H) 7.28−7.40 (m, 2 H) 7.73 (dd, J = 8.6, 2.3 Hz, 1 H) 7.99 (d, J = 2.0 Hz, 1 H) 8.29 (d, J = 8.6 Hz, 1 H) 8.67 (s, 1 H). HRMS: calcd for $C_{20}H_{18}ClF_4N_5O_2S$ $[M+H]^+$, 504.0879; found 504.0878.

(2*R*)-3-Chloro-4-(4-(4-fluoro-2-(trifluoromethyl)phenyl)-2-methylpiperazin-1-ylsulfonyl)phenol (16). A solution of *tert*-butyl ether **14a** (836.0 mg) and trifluoroacetic acid (5 mL) in CH_2Cl_2 (5 mL) was stirred at rt for 6 h. The solvent was evaporated under vacuum, affording the desired product as a white solid (760.0 mg) in 99% yield and used without further purification. ^{1}H NMR (400 MHz, DMSO-d_6) δ 1.21 (d, J = 6.6 Hz, 3H), 2.66−2.74 (m, 2H), 2.83 (d, J = 12.6 Hz, 1H), 2.98 (dd, J = 3.8, 11.4 Hz, 1H), 3.55 (d, J = 13.1 Hz, 1H), 3.93−4.06 (m, 1H), 6.88 (dd, J = 2.4, 8.7 Hz, 1H), 7.03 (d, J = 2.5 Hz, 1H),7.49−7.58 (m, 2H), 7.62 (dd, J = 5.0, 8.8 Hz, 1H), 7.87 (d, J = 8.6 Hz, 1H). HRMS: calcd for $C_{18}H_{17}ClF_4N_2O_3S$ $[M+H]^+$, 453.0657; found 453.0660.

(2*R*)-1-(2-Chloro-4-(difluoromethoxy)phenylsulfonyl)-4-(4-fluoro-2-(trifluoromethyl)phenyl)-2-methylpiperazine (17). A solution of phenol **16** (50.0 mg, 0.11 mmol), $CsCO_3$ (143.0 mg, 0.44 mmol), and methyl-2-chloro-2,2-difluoroacetate (23.0 μL, 0.22 mmol) in DMF/water (4:1) was heated to 120 °C under microwave conditions for 3 h, after which the reaction was judged complete by LCMS. The solution was diluted with ethyl acetate, washed with saturated $NaHCO_3$, and dried over Na_2SO_4. The crude product was purified via silica gel column chromatography, affording 17.0 mg (31%) of the desired compound. ^{1}H NMR (400 MHz, DMSO-d_6) δ ppm 2.60−2.76 (m, 2 H) 2.85 (d, J = 10.9 Hz, 1 H) 2.99 (d, J = 8.1 Hz, 2 H) 3.27−3.41 (m, 1 H) 3.61 (d, J = 13.1 Hz, 1 H) 3.98−4.10 (m, J = 6.9 Hz, 2 H) 7.36 (dd, J = 8.5, 2.4 Hz, 1 H) 7.48 (s, 1 H) 7.50−7.58 (m, 2 H)

7.58−7.70 (m, 1 H) 8.11 (d, J = 8.8 Hz, 1 H). HRMS: calcd for $C_{19}H_{17}ClF_6N_2O_3S$ $[M+H]^+$, 503.0625; found 503.0628.

(2*R*)-1-(2-Chloro-4-ethoxyphenylsulfonyl)-4-(4-fluoro-2-(trifluoromethyl)phenyl)-2-methylpiperazine (18a). To a solution of DEAD (350.0 mg, 2.00 mmol) in anhydrous THF (12.0 mL) was added triphenylphosphine, (510.0 mg, 2.00 mmol. The reaction was stirred for 5 min, and a solution of the phenol **16** (500.0 mg, 1.20 mmol) in THF was added under N_2. The reaction was stirred for 1 h, after which it was judged complete by TLC. The reaction was directly loaded onto a silica gel column and eluted under a gradient of 0−15% MeOH/CH_2Cl_2, affording the desired product as colorless oil (120.0 mg) in 22% yield. ^{1}H NMR (400 MHz, DMSO-d_6) δ ppm 1.22 (d, J = 6.8 Hz, 3 H) 1.35 (t, J = 7.0 Hz, 3 H) 2.58−2.76 (m, 2 H) 2.76−2.90 (m, 1 H) 2.98 (d, J = 7.8 Hz, 1 H) 3.32 (s, 3 H) 3.35−3.42 (m, J = 3.3 Hz, 1 H) 3.57 (d, J = 12.9 Hz, 1 H) 3.89−4.09 (m, 1 H) 4.16 (q, J = 7.0 Hz, 2 H) 7.08 (dd, J = 8.8, 2.5 Hz, 1 H) 7.27 (d, J = 2.5 Hz, 1 H) 7.45−7.70 (m, 3 H) 7.96 (d, J = 8.8 Hz, 1 H). HRMS: calcd for $C_{20}H_{21}ClF_4N_2O_3S$ $[M+H]^+$, 481.0970; found 481.0973.

(2*R*)-1-(2-Chloro-4-(2-methoxyethoxy)phenylsulfonyl)-4-(4-fluoro-2-(trifluoromethyl)phenyl)-2-methylpiperazine (18b). Prepared according to the procedure for compound **18a**, with the exception of the addition of 2-methoxyethanol to the reaction mixture 5 min before the addition of phenol **16**. The desired product was obtained as a colorless oil (44.0 mg) in 8% yield. ^{1}H NMR (400 MHz, DMSO-d_6) δ ppm 1.22 (d, J = 6.8 Hz, 3 H) 2.63−2.74 (m, 2 H) 2.78−2.88 (m, 1 H) 2.98 (dd, J = 11.4, 3.5 Hz, 1 H) 3.09−3.42 (m, J = 6.1 Hz, 4 H) 3.58 (d, J = 12.6 Hz, 1 H) 3.61−3.73 (m, 2 H) 3.92−4.08 (m, 1 H) 4.12−4.29 (m, 2 H) 7.11 (dd, J = 9.1, 2.5 Hz, 1 H) 7.31 (d, J = 2.5 Hz, 1 H) 7.43−7.67 (m, 4 H) 7.96 (d, J = 8.8 Hz, 1 H). HRMS: calcd for $C_{21}H_{23}ClF_4N_2O_4S$ $[M+H]^+$, 511.1076; found 511.1079.

(2*R*)-2-(3-Chloro-4-(4-(4-fluoro-2-(trifluoromethyl)phenyl)-2-methylpiperazin-1-ylsulfonyl)phenoxy)-*N*,*N*-dimethylethanamine (18c). Prepared according to the procedure for compound **18a**, with the exception of the addition of 2-*N*,*N*-dimethylaminoethanol to the reaction mixture 5 min before the addition of phenol **16**. The desired product was obtained as a colorless oil (69.0 mg) in 8% yield. ^{1}H NMR (400 MHz, DMSO-d_6) δ ppm 1.22 (d, J = 6.8 Hz, 3 H) 2.21 (s, 6 H) 2.60−2.75 (m, 4 H) 2.81−2.87 (m, 1 H) 2.94−3.02 (m, 1 H) 3.27−3.39 (m, 1 H) 3.57 (d, J = 15.2 Hz, 1 H) 4.02 (d, J = 5.3 Hz, 1 H) 4.18 (t, J = 5.6 Hz, 2 H) 7.10 (dd, J = 8.8, 2.5 Hz, 1 H) 7.30 (d, J = 2.5 Hz, 1 H) 7.49−7.65 (m, 3 H) 7.96 (d, J = 8.8 Hz, 1 H). HRMS: calcd for $C_{22}H_{26}ClF_4N_3O_3S$ $[M+H]^+$, 524.1392; found 524.1406.

(2*R*)-3-Chloro-4-(4-(4-fluoro-2-(trifluoromethyl)phenyl)-2-methylpiperazin-1-ylsulfonyl)benzonitrile (19). Prepared according to general procedure A, using **5** (6.04 g, 23.01 mmol), 2-chloro-4-cyanobenzene-1-sulfonyl chloride (4.9 mg, 20.92 mmol), and diisopropylethylamine (11.0 mL, 62.76 mmol). The compound was obtained a white solid (5.22 g), in 54% yield. ^{1}H NMR ($CDCl_3$, 400 MHz) δ ppm 1.36 (d, J = 6.8 Hz, 3 H), 2.66−2.84 (m, 2 H), 2.87−3.02 (m, 1 H), 3.07 (dd, J = 11.1, 3.5 Hz, 1 H), 3.47−3.66 (m, 1 H), 3.74 (d, J = 13.1 Hz, 1 H), 4.05−4.22 (m, 1 H), 7.18−7.30 (m, 1 H), 7.29−7.40 (m, 2 H), 7.70 (dd, J = 8.2, 1.6 Hz, 1 H), 7.84 (d, J = 1.5 Hz, 1 H), 8.26 (d, J = 8.1 Hz, 1 H). HRMS: calcd for $C_{19}H_{16}ClF_4N_3O_2S$ $[M+H]^+$, 462.0661; found 462.0661.

(2*R*)-3-Chloro-4-({(2*R*)-4-[4-fluoro-2-(trifluoromethyl)phenyl]-2-methylpiperazin-1-yl}sulfonyl)benzamide (20). To a solution of **19** (11.52 g, 24.99 mmol) in *t*-BuOH (150 mL) was added KOH (7.01 g, 124.93 mmol). The reaction mixture was heated at 65 °C for 2 min and then diluted with EtOAc (300 mL) and washed with water (2 × 150 mL) and then brine (150 mL). The organic layer was dried over $MgSO_4$; the filtrate was concentrated and purified by silica gel column chromatography eluted with ethyl acetate/hexanes (30−50%) to give the title compound as a white solid (9.66 g) in 81% yield. ^{1}H NMR ($CDCl_3$, 400 MHz): δ ppm 1.35 (d, J = 6.8 Hz, 3 H), 2.72−2.83 (m, 2 H), 2.85−2.97 (m, 1 H), 3.06 (dd, J = 11.1, 3.5 Hz, 1 H), 3.50−3.65 (m, 1 H), 3.73 (d, J = 13.1 Hz, 1 H), 4.12−4.19 (m, 1 H), 5.89 (br s, 1 H), 6.20 (br s, 1 H), 7.17−7.29 (m, 1 H), 7.29−7.39 (m, 2 H), 7.77 (dd, J = 8.2, 1.6 Hz, 1 H), 8.00 (d, J = 1.8 Hz, 1 H), 8.20 (d, J = 8.1 Hz, 1 H). HRMS: calcd for $[C_{19}H_{18}ClF_4N_3O_3S+Na]^+$, 502.0586; found 502.0586.

Cellular Assays. Determination of IC_{50} against Human 11β-HSD1. Compounds described herein were tested in a cell-based assay using a stable Chinese hamster ovary (CHO) cell line expressing human 11β-HSD1. Cells were plated at 20000 cells/well in 384-well plates and incubated overnight (12−16 h) at 37 °C/5% CO_2. Cells were treated with different concentration of compound in 90 μL of serum-free media and incubated for 30 min at 37 °C/5%CO_2. Cortisone (10 μL of 5 μM, final concentration 500 nM) was then added to the cells and the plate was incubated at 37 °C/5%CO_2 for 120 min. Then 15 μL of media was withdrawn and the amount of cortisol in the media was measured using the DiscoverX HitHunter cortisol assay (DiscoverX corp, CA), following manufacturer's instructions. Briefly, 15 μL media was transferred to a white 384-well assay plate. Then 5 μL of anticortisol antibody and 10 μL of enzyme donor (ED) complex were added to each well of the assay plate. The assay plate was incubated at rt for 60 min with gentle shaking. Galacton Star, Emerald Green, and chemiluminescence substrate buffer were mixed 1:5:19. The mixture was then combined in equal parts with enzyme acceptor (EA) complex. Then 20 μL of the mix was added to each well of the assay plate and the assay plate was incubated at room temperature for another 60 min. The plate was read in Envision multilabel plate reader (Perkin-Elmer, MA) in the enhanced luminescence mode. Background subtracted data was fitted to $y = a+(b/(1+x/IC_{50}))$, and IC_{50} values were calculated using XLFit (IDBS, MA).

Determination of IC_{50} against Mouse 11β-HSD1. To determine the IC_{50} against mouse 11β-HSD1, a stable CHO cell line expressing mouse 11β-HSD1 was used and the above procedure was followed.

Determination of IC_{50} against Mouse 11β-HSD1 in the Presence of Serum. To determine the IC_{50} against mouse 11β-HSD1 in the presence of serum, 10% defibrinated, delipidized, charcoal stripped human serum (Seracare Life Sciences, CA) was added during the incubation with compound and cortisone. The above procedure was followed.

Evaluation of Inhibition of Human 11β-HSD2. To determine the potency of compounds against mouse 11β-HSD2, a stable CHO cell line expressing human 11β-HSD2 is generated. Cells were plated at 20000 cells/well in 96-well plates and incubated overnight (12−16 h) at 37 °C/5% CO_2. Cells were treated with different concentration of compound in 90 μL of serum-free media and incubated for 30 min at 37 °C/5%CO_2. Then 10 μL of 500 nM [^{3}H]-Cortisone (ARC Inc., MO) was added to each well of the plate (final concentration = 50 nM). The plate was incubated for 120 min. Cortisone and cortisol were separated on a PRP-1 (Hamilton Inc., NV) on an Agilent 1100 high pressure liquid chromatography system with a 500TR flow scintillation analyzer (Perkin-Elmer, MA). Carbenoxolone (Sigma, MO) was used as a control 11β-HSD2 inhibitor.

Evaluation of 11β-HSD1 Inhibitors in Mouse ex Vivo Assay. To characterize the inhibitors of 11β-HSD1, inhibitors were tested in mouse tissue ex vivo assay. Male C57Bl6 mice 8−10 weeks of age were grouped based on body weight (Taconic Farms on standard chow diet). The compounds were suspended in 0.5% methyl cellulose/2%tween in water. All mice were orally dosed and sacrificed 2−5 h after dosing (n = 4). Liver and epididymal fat tissues were collected and frozen in liquid nitrogen. Tissue 11β-HSD1 ex vivo assay measured the conversion of [^{3}H]-cortisone to [^{3}H]-cortisol, and percent inhibition of 11β-HSD1 activity in the liver was determined in reference to vehicle treated mice. then 50−60 mg of frozen liver tissue was placed in 48-well plates (kept on dry ice). The tissue/48-well plates were thawed at rt for 15 min, and then 250 μL of PBS were added to each well and incubated for additional 15 min at rt. The 48-well plate was placed on a 37 °C Eppendorf Thermomixer R plate shaker, and 250 μL of PBS containing 2.5 μCi of [^{3}H]-cortisone

was added to each well and allowed to incubate for 30 min. The reaction was stopped by adding 50 μL of 10% TFA. Reaction aliquot (20 μL) was analyzed by HPLC and percent conversion of [^{3}H]-cortisone to [^{3}H]-cortisol determined (t test, *$p < 0.05$).

Evaluation of 11β-HSD1 Inhibitors in Mouse ex Vivo Assay with Food Mix. All experimental protocol was approved by the Institutional Animal Care and Use Committee of Wyeth Research. Diet induced obese mice were individually housed and maintained under 12L:12D cycle (6 a.m./6 p.m.). Prior to implementing the long-term efficacy study, we evaluated the properties of 11β-HSD-1 inhibitor when mixed with high fat diet (Research Diet D12492). Two weeks prior to initiation of dosing regimen, one-half of 18 weeks old C57B6 DIO mice that had been on a high fat diet for 12 weeks from Taconic were placed in reversed light cycle room (remaining one-half in normal light cycle, where mice were subjected to a 14 h shift in light cycle (dark cycle began on 8 a.m. and light cycle began on 8 p.m.). This ensured that blood and tissue collection could take place during normal light cycle from 6 a.m. to 6 p.m. Diurnal rhythm in the feeding behavior of rodents dictated that these nocturnal animals consumed majority of the food during the corresponding dark phase. The peak feeding time for the nocturnal rodents were at on set of darkness; therefore theoretical peak for the compound concentration in serum was estimated to occur 4 h after lights off (10 a.m.). Likewise, rodent food intake dramatically decreased at the onset of light; therefore we estimated that the theoretical low for the compound concentration in serum to occur 4 h after lights on (10 p.m.). C57Bl6 DIO mice were fed with food mixed with compounds at 0.5 mg/g food for 96 h. The mice that were under normal light cycle condition were sacrificed at 10 a.m. (Table 7, day 4, 10 a.m.) and mice that under reverse light cycle were sacrificed at 12 p.m. (Table 7, day 4, 10 p.m.). The fat and liver tissues were collected. The drug concentration was determined by HPLC analysis, and liver food mix ex vivo was conducted as discussed. For all studies, compounds were sent to Research Diet and compound/food mixture was prepared according to Research Diet Standard Operation Procedure. The results are expressed in ng/mL for serum and ng/g for liver and fat. Each value represents mean ± SEM of mice (n = 6). The data was analyzed by performing t test with two-tail distribution, two-sample unequal variance and asterisks indicate statistical significance at $p < 0.05$ vs vehicle.

X-Ray Crystallographic Studies Including Protocol for Getting and Resolving X-Ray Structures. 11β-HSD1 residues 24-292 C272S was prepared in the presence of CHAPS as described.[21] Crystals were grown using the hanging drop method with a reservoir solution of 100 mM HEPES pH 6.8−7.1 and 16−18% PEG 3350. Crystals were soaked from 1−3 d in reservoir solution containing compound at 0.5−1 mM, and 0.1% glutaraldehyde was added to the well to stabilize the crystals during soaking. The crystals were cryoprotected in paratone oil and flash frozen in a cryo-stream. X-ray data was collected using a Rigaku FR-E X-ray generator and a Rigaku Saturn92 CCD detector. Data was reduced using HKL2000.[22] The structure was solved by using phenix.refine[23] for rigid body fitting of the published structure of HSD1 with CHAPS (1XU9). Each protein chain was treated as an independent rigid body. The structure was refined through iterative manual rebuilding and reciprocal space refinement using COOT[24] and phenix.refine. The structure was further validated using Molprobity.[25]

Pharmacokinetic and Metabolic Stability Studies. Pharmacokinetics of 11β-HSD1 inhibitors was determined in male C57/B6 mice (20−30 g, Taconic Farm, NY) after iv or po administration. The compounds were prepared in DSM/PEG-200/saline solution for the iv administration or in 0.5% MC/2% TW/water as a suspension for the po administration. Blood samples were collected over a period of 24 h, and plasma samples were harvested and stored at −80 °C until assay. The target tissues (liver and muscle) were also collected at selected time points. Tissues were homogenized in saline, and the drug concentrations in the homogenates were analyzed. Quantization of HSD1 inhibitors in plasma and tissue homogenate was carried with a verified LC/MS/MS method.

In vitro metabolic half-life ($t_{1/2}$) and metabolic pathways were determined in liver microsomes from rats, mice, and humans using an NADPH regenerating system consisting of $MgCl_2$ (10 mM), glucose-6-phosphate (3.6 mM), $NADP^+$ (1.3 mM), and glucose-6-phosphate dehydrogenase (0.4 units/mL) in sodium phosphate buffer (0.1 M, pH 7.4), UDPGA (4 mM), and substrate (1 mM for metabolic stability and 10 mM for metabolite profiling). Incubations were initiated by the addition of the NADPH generating system and conducted for up to 30 min in a shaker-water bath at 37 °C. For the determination of in vitro metabolic half-life, aliquots of the incubation mixture were removed at 0, 10, 20, and 30 min and added to acetonitrile containing the appropriate internal standard. Following centrifugation and evaporation of the supernatant liquid, the samples were reconstituted in 20% methanol in water for analysis by LC/MS.

In Vivo Study through Food Mix. male DIO-B6 mice, 26 weeks old (Taconic, Diet D12492, 60% fat, n = 12), were used to evaluate in vitro efficacy of compound **20** in this reversal model. The mice were grouped based on body weight and serum insulin levels and placed one per cage and fed on high fat diet (60% fat kcal, 35.5% fat, F1850, BioServ, paste formula of no. 3282) 7 weeks prior start of the study. A food mix was prepared by mixing 0.5 mg of compound **20** with 1 g of the high fat diet (prepared by Research Diet). The mice were fed with this mixture for 31 days. Body weights and food intake were weekly measured. Fed glucose and insulin levels were obtained at day 21, and fasting glucose and insulin levels were obtained at day 26 by tail bleeding. To minimize the effects of stress induced fasting, fed glucose and insulin values were first recorded and then 5 days later fasting values were obtained. Mice were sacrificed under "stress free" conditions at the end of study, and serum and tissues were collected and frozen in liquid nitrogen. Serum and tissues were collected for analysis. The results (Figures 4 and 5) are expressed in ng/mL for insulin and mg/dL for glucose . Each value represents mean ± SEM of mice (n = 12). The data was analyzed by performing t test with two-tail distribution, two-sample unequal variance, and asterisks indicate statistical significance at $p < 0.05$ vs vehicle.

Acknowledgment. We thank Nelson Huang, Ning Pan, Peter Tate, Walter Massefski, and Li Di for coordinating and obtaining analytical data, and Katherine Lee for proof reading of this manuscript.

Note Added after ASAP Publication. This paper was published on August 10, 2009 with an incorrect spelling of an author name. The revised version was published on August 12, 2009.

References

(1) Zimmet, P. Z.; Alberti, K. G.; Shaw, J. Global and societal implications of the diabetes epidemic. *Nature* **2001**, *414*, 782–787.
(2) Day, C. Metabolic syndrome, or what you will: definitions and epidemiology. *Diabetes Vasc. Dis. Res.* **2007**, *4*, 32–38.
(3) Mohler, M. L.; He, Y.; Wu, Z.; Hwang, D. J.; Miller, D. D. Recent and emerging anti-diabetes targets. *Med. Res. Rev.* **2009**, *29*, 125–195.
(4) (a) Tomlinson, J. W.; Walker, E. A.; Bujalska, I. J.; Draper, N.; Lavery, G. G.; Cooper, M. S.; Hewison, M.; Stewart, P. M. 11β-Hydroxysteroid dehydrogenase type 1: a tissue-specific regulator of glucocorticoid response. *Endocr. Rev.* **2004**, *25*, 831–866. (b) Stulnig, T. M.; Waldhausl, W. 11β-Hydroxysteroid dehydrogenase type 1 in obesity and type 2 diabetes. *Diabetologia* **2004**, *47*, 1–11.
(5) (a) Masuzaki, H.; Peterson, J.; Shinyama, H.; Morton, N. M.; Mullins, J. J.; Seckl, J. R.; Flier, J. S. A transgenic model of visceral obesity and the metabolic syndrome. *Science* **2001**, *294*, 2166–2170. (b) Masuzaki, H.; Yamamoto, H.; Kenyon, C. J.; Elmquist, J. K.; Morton, N. M.; Paterson, M. M.; Shinyama, H.; Sharp, M. G.; Fleming, S.; Mullins, J. J.; Seckl, J. R.; Flier, J. S. Transgenic amplification of glucocorticoid action in adipose tissue causes high blood pressure in mice. *J. Clin. Invest.* **2003**, *112*, 83–88.

(6) Paterson, J. M.; Morton, N. M.; Fievet, C.; Kenyon, C. J.; Holmes, M. C.; Staels, B.; Seckl, J. R.; Mullins, J. J. Metabolic syndrome without obesity: hepatic overexpression of 11*β*-hydroxysteroid dehydrogenase type 1 in transgenic mice. *Proc. Natl. Acad. Sci. U.S.A.* **2004**, *101*, 7088–7093.

(7) Morton, N. M.; Paterson, M.; Masuzaki, H.; Holmes, M.; Staels, B.; Fievet, C.; Walker, B.; Flier, J. S.; Mullins, J. J.; Seckl, J. R. Novel adipose tissue- mediated resistance to diet-induced visceral obesity in 11*β*-hydroxysteroid dehydrogenase type-1 deficient mice. *Diabetes* **2004**, *53*, 931–938.

(8) For a review, see: (a) Saiah, E. The role of 11beta-hydroxysteroid dehydrogenase in metabolic disease and therapeutic potential of 11beta-HSD1 inhibitors. *Curr. Med. Chem.* **2008**, *15*, 642–649Recently reported 11β-HSD1 inhibitors: . (b) Sun, D.; Wang, Z.; Di, Y.; Jaen, J. C.; Labelle, M.; Ma, J.; Miao, S.; Sudom, A.; Tang, L.; Tooka, C. S.; Tu, H.; Ursu, S.; Walker, N.; Yan, X.; Ye, Q.; Powers, J. P. Discovery and Initial SAR of Arylsulfonylpiperazine Inhibitors of 11β-Hydroxysteroid Dehydrogenase Type 1 (11β-HSD1). *Bioorg. Med. Chem. Lett.* **2008**, *18*, 3513–3516. (c) Aster, S. D.; Graham, D. W.; Kharbanda, D.; Patel, G.; Ponpipom, M.; Santorelli, G. M.; Szymonifka, M. J.; Mundt, S. S.; Shah, K.; Springer, M. S.; Thieringer, R.; Hermanowski-Vosatka, A.; Wright, S. D.; Xiao, J.; Zokian, H.; Balkovec, J. M. Bisaryl triazoles as selective inhibitors of 11β-hydroxysteroid dehydrogenase type 1. *Bioorg. Med. Chem. Lett.* **2008**, *18*, 2799–2804. (d) St. Jean, D. J.; Yuan, C.; Bercot, E. A.; Cupples, R.; Chen, M.; Fretland, J.; Hale, C.; Hungate, R. W.; Komorowski, R.; Veniant, M.; Wang, M.; Zhang, X.; Fotsch, C. 2-(*S*)-Phenethylaminothiazolones as potent, orally efficacious inhibitors of 11β-hydroxysteroid dehydrogenase type 1. *J. Med. Chem.* **2007**, *50*, 429–432. (e) Rohde, J. J.; Pliushchev, M. A.; Sorensen, B. K.; Wodka, D.; Shuai, Q.; Wang, J.; Fung, S.; Monzon, K. M.; Chiou, W. J.; Pan, L.; Deng, X.; Chovan, L. E.; Ramaiya, A.; Mullally, M.; Henry, R. F.; Stolarik, D. F.; Imade, H. M.; Marsh, K. C.; Beno, D. W. A.; Fey; Thomas, A.; Droz, B. A.; Brune, M. E.; Camp, H. S.; Sham, H. L.; Frevert, E. U.; Jacobson, P. B.; Link, J. T. Discovery and metabolic stabilization of potent and selective 2-amino-N-(adamant-2-yl)acetamide 11β-hydroxysteroid dehydrogenase type 1 inhibitors. *J. Med. Chem.* **2007**, *50*, 149–164. (f) Xiang, J.; Ipek, M.; Suri, V.; Tam, M.; Xing, Y.; Huang, N.; Zhang, Y.; Tobin, J.; Mansour, T.; McKew, J. β-Keto sulfones as inhibitors of 11β-hydroxysteroid dehydrogenase type 1 and the mechanism of action. *Bioorg. Med. Chem.* **2007**, *15*, 4396–4405. (g) Sorensen, B.; Winn, M.; Rohde, J.; Shuai, Q.; Wang, J.; Fung, S.; Monzon, K.; Chiou, W.; Stolarik, D.; Imade, H.; Pan, L.; Deng, X.; Chovan, L.; Longenecker, K.; Judge, R.; Qin, W.; Brune, M.; Camp, H.; Frevert, E. U.; Jackbson, P.; Link, J. T. Adamantane sulfone and sulfonamide 11β-HSD1 inhibitors. *Bioorg. Med. Chem. Lett.* **2007**, *17*, 527–32. (h) Yeh, V.; Kurukulasuriya, R.; Madar, D.; Patel, J.; Fung, S.; Monzon, K.; Chiou, W.; Wang, J.; Jacobson, P.; Sham, H.; Link, J. Synthesis and structural activity relationship of 11β-HSD1 inhibitors with novel adamantane replacements. *Bioorg. Med. Chem. Lett.* **2006**, *16*, 5408–5413. (i) Schuster, D.; Maurer, E.; Laggner, C.; Nashev, L.; Wilckens, T.; Langer, T.; Odermatt, A. The discovery of new 11β-hydroxysteroid dehydrogenase type 1 inhibitors by common feature pharmacophore modeling and virtual screening. *J. Med. Chem.* **2006**, *49*, 3454–3466. (j) Gu, X.; Dragovic, J.; Koo, G. C.; Koprak, S. L.; LeGrand, C.; Mundt, S. S.; Shah, K.; Springer, M.; Tan, E.; Thieringer, R.; Hermanowski- Vosatka, A.; Zokian, H.; Balkovec, J.; Waddell, S. T. Discovery of 4-heteroarylbicyclo[2.2.2]octyltriazoles as potent and selective inhibitors of 11β-HSD1: Novel therapeutic agents for the treatment of metabolic syndrome. *Bioorg. Med. Chem. Lett.* **2005**, *15*, 5266–5269. (k) Olson, S.; Aster, S.; Brown, K.; Carbin, L.; Graham, D.; Hermanowski, A.; LeGrand, C.; Mundt, S.; Robbins, M.; Schaeffer, J.; Slossberg, L.; Szymonifka, M.; Thieringer, R.; Wright, S.; Balkovec, J. Adamantyl triazoles as selective inhibitors of 11β-hydroxysteroid dehydrogenase type 1. *Bioorg. Med. Chem. Lett.* **2005**, *15*, 4359–4362. (l) Xiang, J.; Ipek, M.; Suri, V.; Massefski, W.; Pan, N.; Ge, Y.; Tam, M.; Xing, Y.; Tobin, J.; Xu, X.; Tam, S. Synthesis and biological evaluation of sulfonamidooxazoles and β-keto sulfones: selective inhibitors of 11β-hydroxysteroid dehydrogenase type I. *Bioorg. Med. Chem. Lett.* **2005**, *15*, 2865–2869. (m) Coppola, G.; Kukkola, P.; Stanton, J.; Neubert, A.; Marcopulos, N.; Bilci, N.; Wang, H.; Tomaselle, H.; Tan, J.; Aicher, T.; Knorr, D.; Jeng, A.; Dardik, B.; Chatelain, R. Perhydroquinolylbenzamides as novel inhibitors of 11β-hydroxysteroid dehydrogenase type 1. *J. Med. Chem.* **2005**, *48*, 6696–6712.

(9) (a) Barf, T.; Vallgarda, J.; Emond, R.; Haggstrom, C.; Kurz, G.; Nygren, A.; Larwood, V.; Mosialou, E.; Axelsson, K.; Olsson, R.; Engblom, L.; Edling, N.; Ronquist-Nii, Y.; Ohman, B.; Alberts, P.; Abrahmsen, L. Arylsulfonamidothiazoles as a new class of potential antidiabetic drugs: discovery of potent and selective inhibitors of the 11β-hydroxysteroid dehydrogenase type 1. *J. Med. Chem.* **2002**, *45*, 3813–3815. (b) Alberts, P.; Engblom, L.; Edling, N.; Forsgren, M.; Klingstrom, G.; Larsson, C.; Ronquist-Nii, Y.; Ohman, B.; Abrahmsen, L. Selective inhibition of 11β-hydroxysteroid dehydrogenase type 1 decreases blood glucose concentrations in hyperglycaemic mice. *Diabetologia* **2002**, *45*, 1528–1532. (c) Alberts, P.; Nilsson, C.; Selen, G.; Engblom, L. O.; Edling, N. H.; Norling, S.; Klingstrom, G.; Larsson, C.; Forsgren, M.; Ashkzari, M.; Nilsson, C. E.; Fiedler, M.; Bergqvist, E.; Ohman, B.; Bjorkstrand, E.; Abrahmsen, L. B. Selective inhibition of 11β-hydroxysteroid dehydrogenase type 1 improves hepatic insulin sensitivity in hyperglycemic mice strains. *Endocrinology* **2003**, *144*, 4755–4762.

(10) Rueckle, T.; Vitte, P. A.; Gotteland, J. P. WO Patent 2005025558, **2005**.

(11) Hermanowski-Vosatka, A.; Balkovec, J. M.; Cheng, K.; Chen, H. Y.; Hernandez, G. C.; Koo, G. C.; LeGrand, C. B.; Li, Z.; Metzger, M. M.; Mundt, S. S.; Noonan, H.; Nunes, C. N.; Olson, S. H.; Pikounis, B.; Ren, N.; Robertson, N.; Schaeffer, M. M.; Shah, K.; Springer, M. S.; Strack, A. M.; Strowski, M.; Wu, K.; Wu, T.; Xiao, J.; Zhang, B. B.; Wright, S. D.; Thieringer, R. 11β-HSD1 inhibition ameliorates metabolic syndrome and prevents progression of atherosclerosis in mice. *J. Exp. Med.* **2005**, *202*, 517–527.

(12) Hoff, E. D.; Link, J. T.; Pliushchev, M. M.; Rohde, J. J.; Winn, M. U.S. Patent 20050245533, **2005**.

(13) Yeh, V. S. C.; Kurukulasuriya, R.; Fung, S.; Monzon, K.; Chiou, W.; Wan, J.; Stolarik, D.; Imade, H.; Shapiro, R.; Knoure-Segel, V.; Bush, E.; Wilcox, D.; Nguyen, H. T.; Brune, M.; Jacobson, P.; Link, J. T. Discovery of orally active butyrolactam 11β-HSD1 inhibitors. *Bioorg. Med. Chem. Lett.* **2006**, *16*, 5555–5560.

(14) Bhat, B. G.; Hosea, N.; Fanjul, A.; Herrera, J.; Chapman, J.; Thalacker, F.; Stewart, P. M.; Rejto, P. A. Demonstration of proof of mechanism and pharmacokinetics and pharmacodynamic relationship with 4′-cyano-biphenyl-4-sulfonic acid (6-amino-pyridin-2-yl)-amide (PF-915275), an inhibitor of 11β-hydroxysteroid dehydrogenase type 1, in cynomolgus monkeys. *J. Pharmacol. Exp. Ther.* **2008**, *324*, 299–305.

(15) Xiang, J.; Wan, Z.-K.; Li, H.-Q.; Ipek, M.; Binnun, E.; Nunez, J.; Chen, L.; McKew, J. C.; Mansour, T. S.; Xu, X.; Suri, V.; Tam, M.; Xing, Y.; Li, X.; Hahm, S.; Tobin, J.; Saiah, E. Piperazine sulfonamides as potent, selective, and orally available 11β-hydroxysteroid dehydrogenase type 1 inhibitors with efficacy in the rat cortisone-induced hyperinsulinemia model. *J. Med. Chem.* **2008**, *51*, 4068–4071.

(16) (a) Wagaw, S.; Buchwald, S. L. The synthesis of aminopyridines: a method employing palladium-catalyzed carbon-nitrogen bond formation. *J. Org. Chem.* **1996**, *61*, 7240–7241. (b) Old, D. W.; Wolfe, J. P.; Wagaw, S.; Marcoux, J.-F.; Buchwald, S. L. Rational development of practical catalysts for aromatic carbon-nitrogen bond formation. *Acc. Chem. Res.* **1998**, *31*, 805–818.

(17) (a) Mune, T.; Rogerson, F. M.; Nikkila, H.; Agarwal, A. K.; White, P. C. Human hypertension caused by mutations in the kidney isoenzyme of 11β-hydroxysteroid dehydrogenase. *Nat. Genet.* **1995**, *10*, 394–399. (b) Dave-Sharma, S.; Wilson, R. C.; Harbison, M. D.; Newfield, R.; Azar, M. R.; Krozowski, Z. S.; Funder, J. W.; Shackleton, C. H. L.; Bradlow, H. L.; Wei, J.-Q.; Hertecant, J.; Moran, A.; Neiberger, R. E.; Balfe, J. W.; Fattah, A.; Daneman, D.; Akkurt, H. I.; De Santis, C.; New, M. I. Examination of genotype and phenotype relationships in 14 patients with apparent mineralocorticoid excess. *J. Clin. Endocrinol. Metab.* **1998**, *83*, 2244–2254.

(18) Manuscript is under preparation.

(19) Adam, T. C.; Epel, E. S. Stress, eating and the reward system. *Physiol. Behav.* **2007**, *91*, 449–458.

(20) Lambillotte, C.; Gilon, P.; Henquin, J. C. Direct glucocorticoid inhibition of insulin secretion. An in vitro study of dexamethasone effects in mouse islets. *J. Clin. Invest.* **1997**, *99*, 414–423.

(21) Hosfield, D. J.; Wu, Y.; Skene, R. J.; Hilgers, M.; Jennings, A.; Snell, G. P.; Aertgeerts, K. Conformational flexibility in crystal structures of human 11β-hydroxysteroid dehydrogenase type I provide insights into glucocorticoid interconversion and enzyme regulation. *J. Biol. Chem.* **2005**, *280*, 4639–4648.

(22) Otwinowski, Z.; Minor, W. Processing of X-ray Diffraction Data Collected in Oscillation Mode. *Methods Enzymol* **1997**, *276*, 307–326.

(23) Adams, P. D.; Grosse-Kunstleve, R. W.; Hung, L.-W.; Ioerger, T. R.; McCoy, A. J.; Moriarty, N. W.; Read, R. J.; Sacchettini, J. C.; Sauter, N. K.; Terwilliger, T. C. PHENIX: building new software for automated crystallographic structure determination. *Acta Crystallogr., Sect. D: Biol. Crystallogr.* **2002**, *58*, 1948–1954.

(24) Emsley, P.; Cowtan, K. Coot: model-building tools for molecular graphics. *Acta Crystallogr., Sect. D: Biol. Crystallogr.* **2004**, *60*, 2126–2132.

(25) Lovell, S. C.; Davis, I. W.; Arendall, W. B., III; de Bakker, P. I. W.; Word, J. M.; Prisant, M. G.; Richardson, J. S.; Richardson, D. C. Structure validation by Cα geometry: ϕ, ψ, and Cβ deviation. *Proteins: Structure, Function, and Genetics* **2003**, *50*, 437–450.

(26) DeLano, W. L. *The PyMOL User's Manual*; DeLano Scientific: Palo Alto, CA, 2002.